Electronic Supplementary Information (ESI)
for
AIE-active cyclometalated iridium(III) complexes for the highly efficient picric acid detection in aqueous media

*Monosh Rabha, Deikrisha Lyngdoh Lyngkhoi, Sumit Kumar Patra, and Snehadrinarayan Khatua**

Department of Chemistry, North-Eastern Hill University, Shillong, Meghalaya 793022, India

***Email:** snehadri@gmail.com; skhatua@nehu.ac.in

Table of Contents

Chart S1. Synthetic schemes and list of compounds.

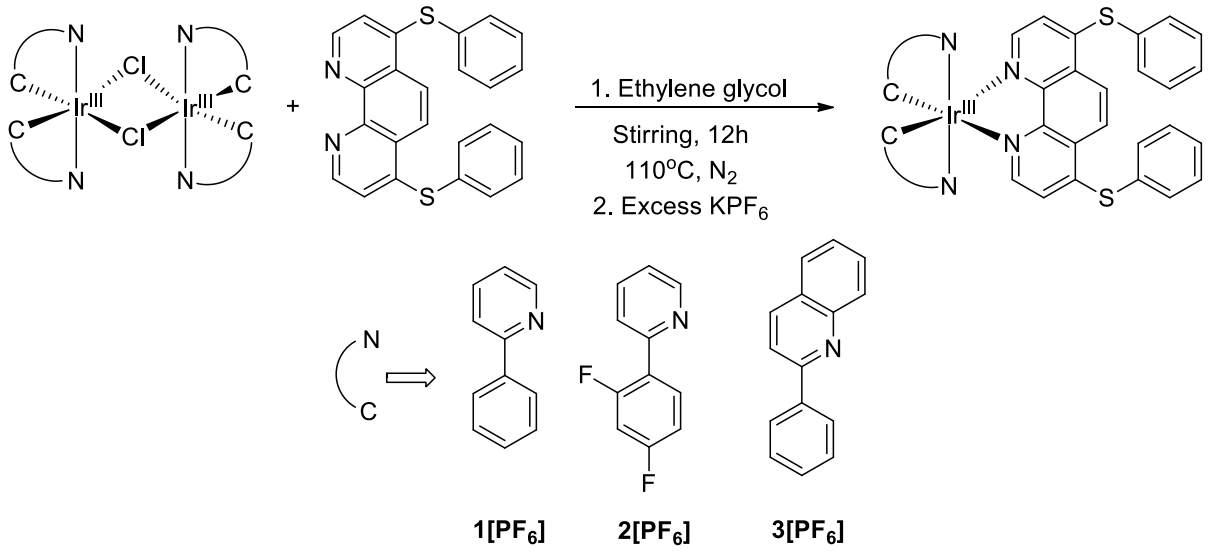

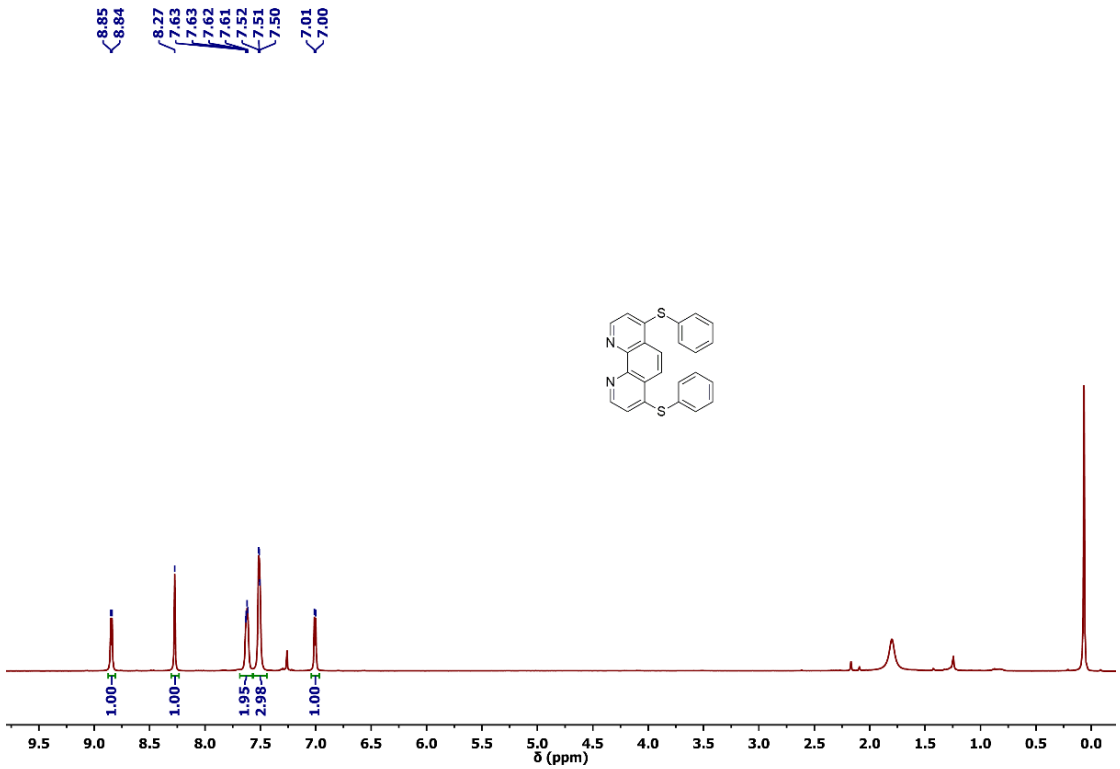

Fig. S1. ^{1}H NMR spectrum of **L** in $CDCl_3$.

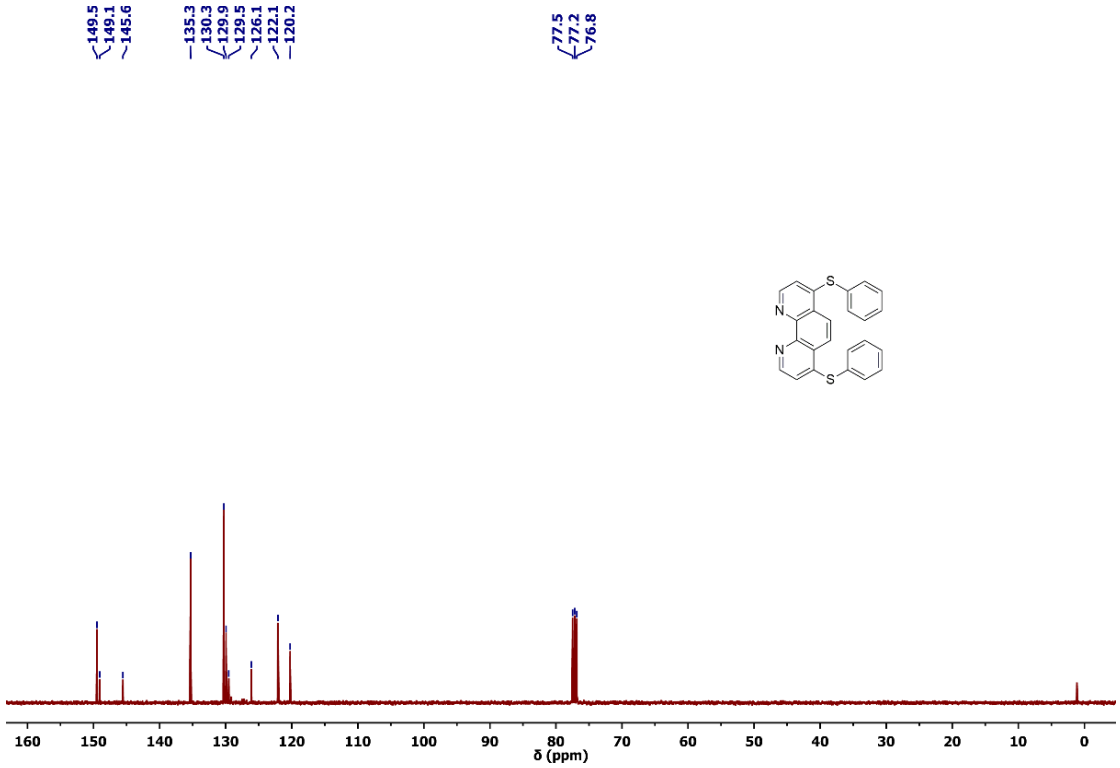

Fig. S2. ^{13}C NMR spectrum of **L** in $CDCl_3$.

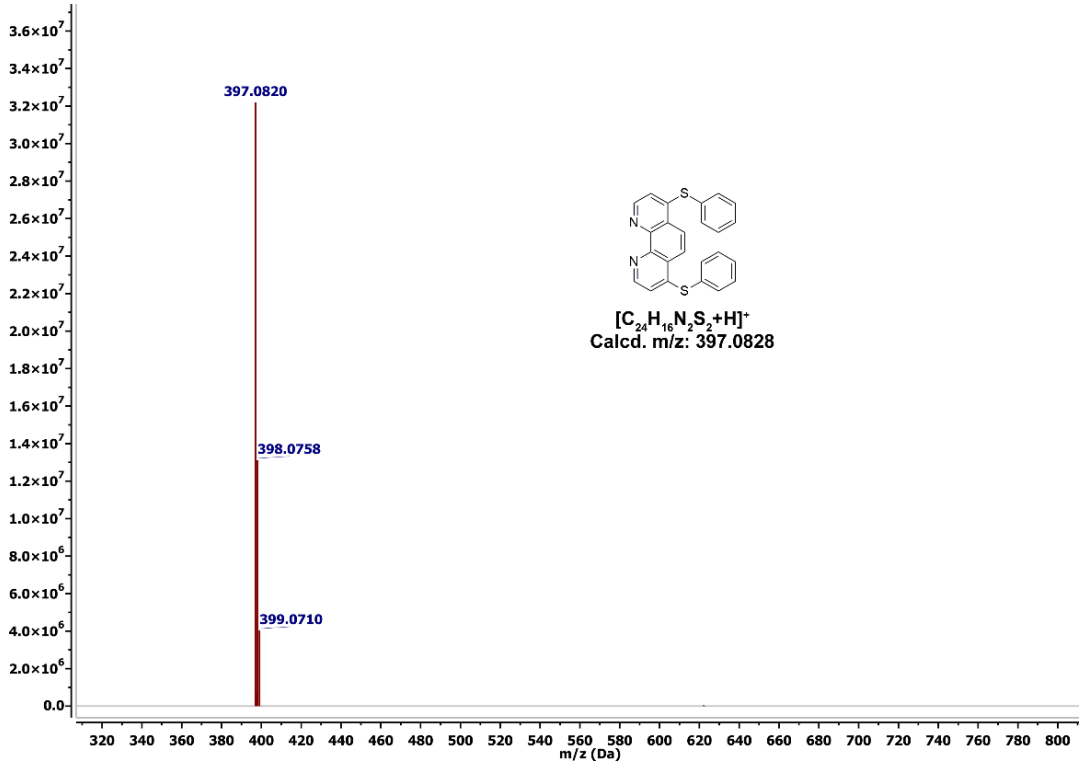

Fig. S3. HRMS spectrum of **L** in methanol.

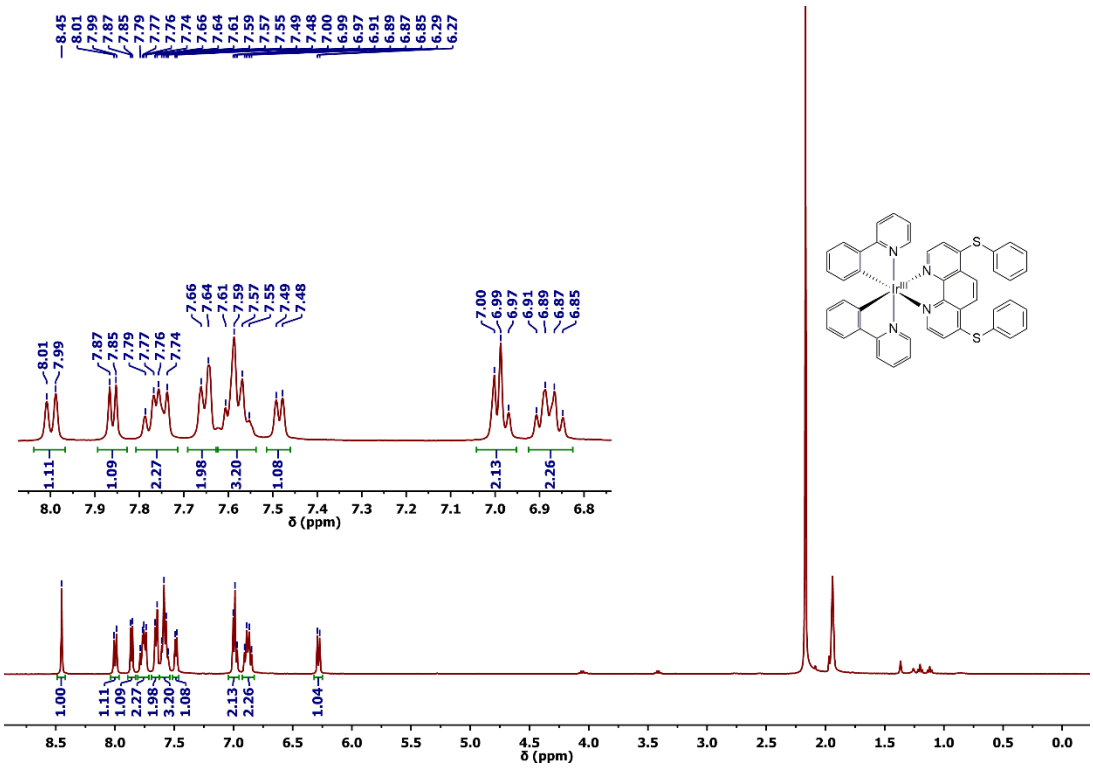

Fig. S4. ^{1}H NMR spectrum of **1[PF$_6$]** in CD_3CN.

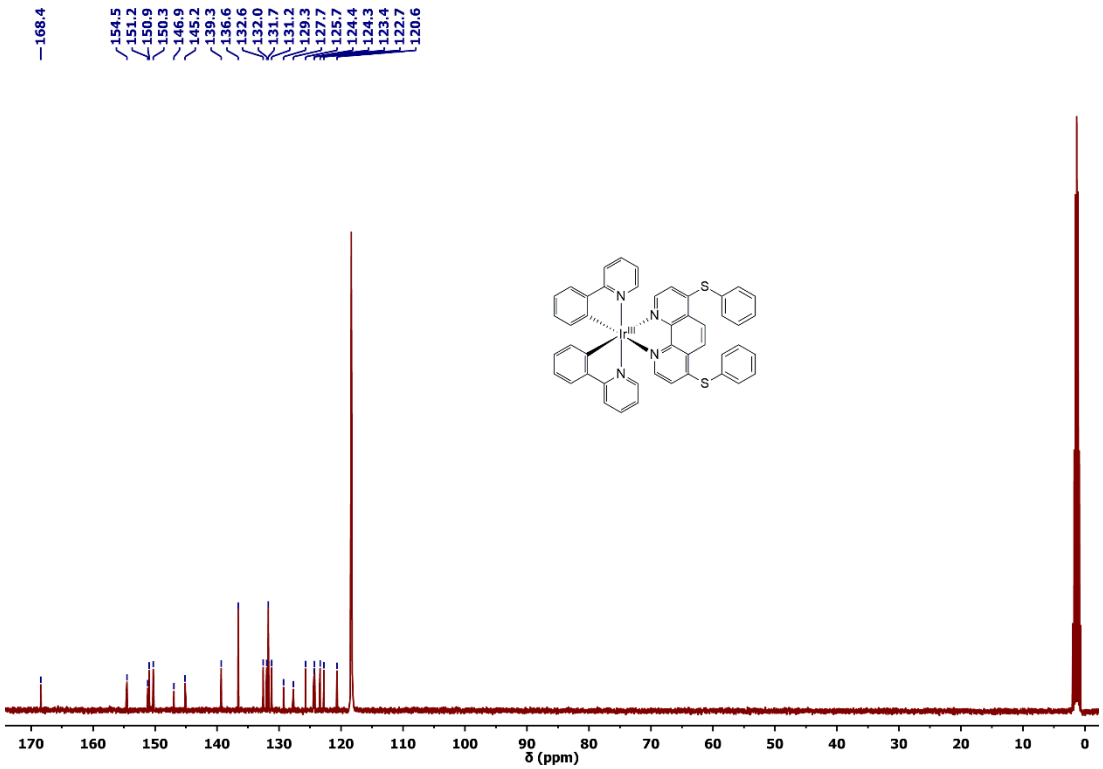

Fig. S5. ^{13}C NMR spectrum of **1[PF$_6$]** in CD_3CN.

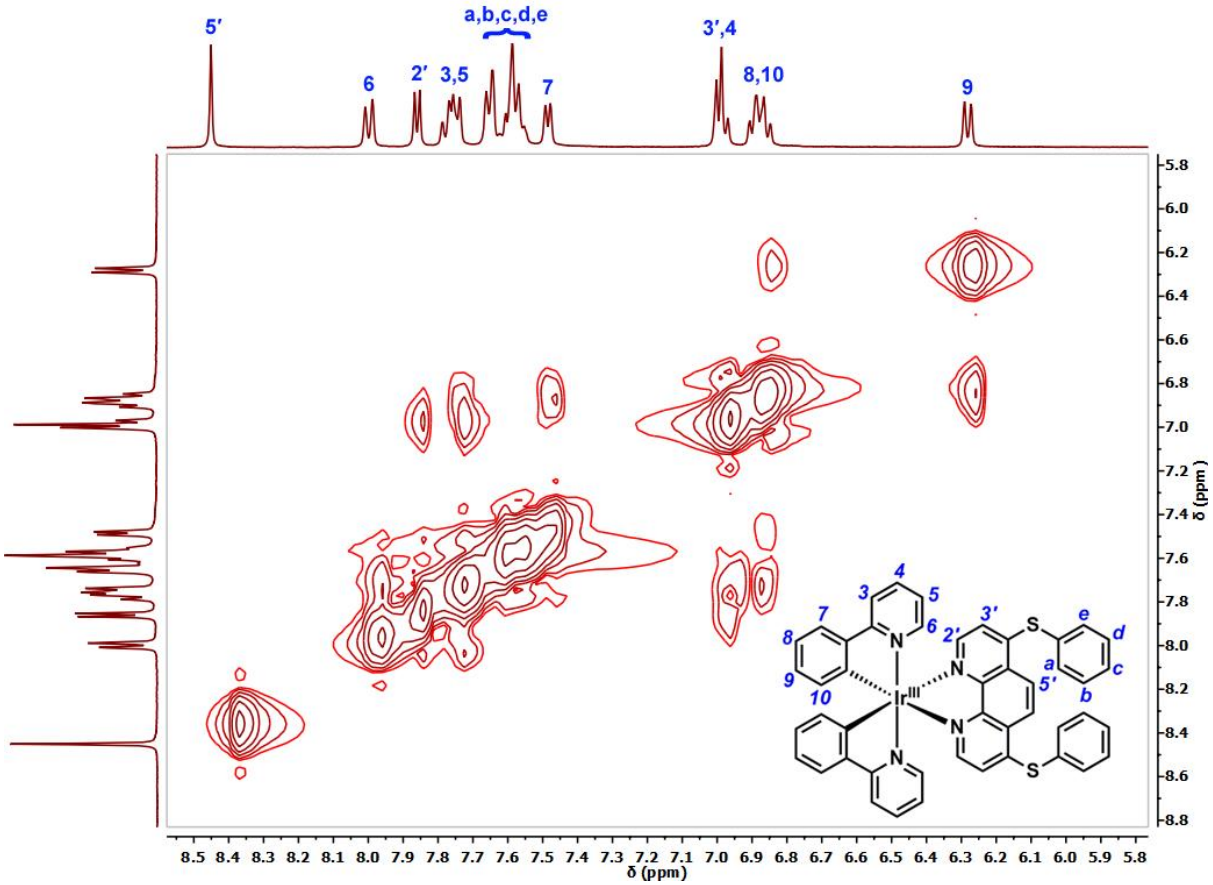

Fig. S6. Partial ^{1}H-^{1}H COSY NMR spectrum of **1[PF$_6$]** in CD_3CN.

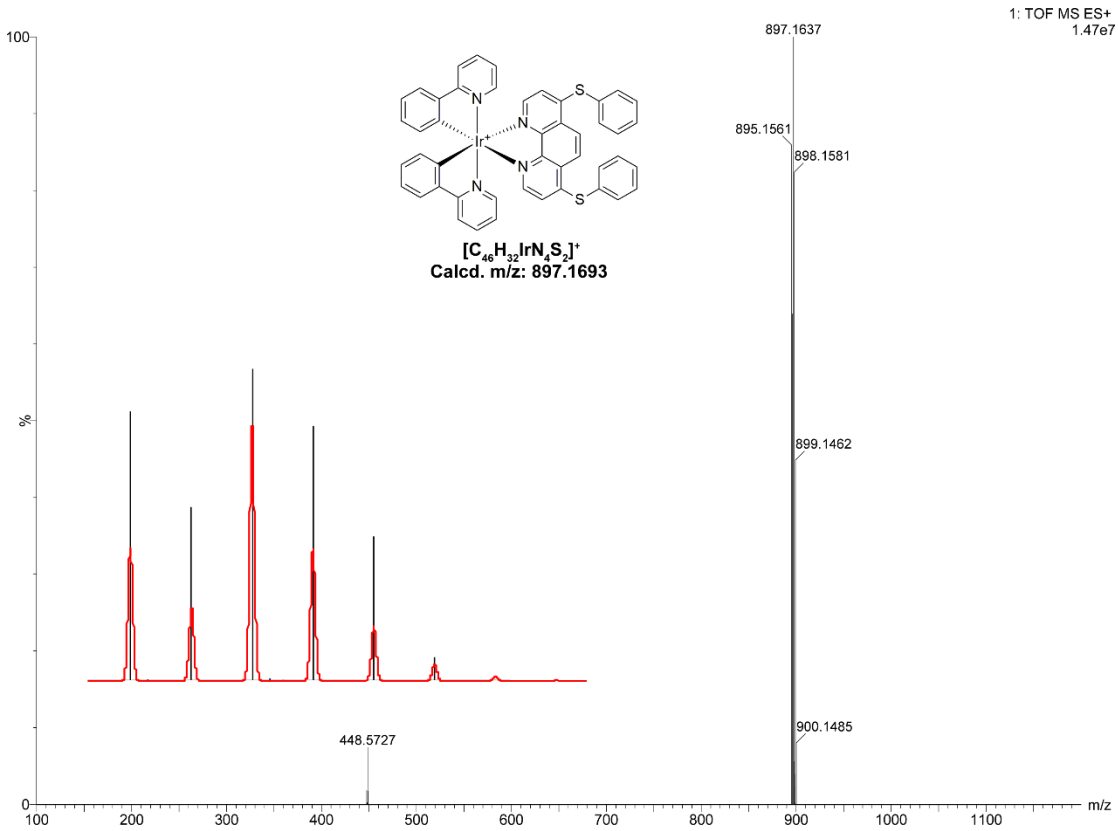

Fig. S7. HRMS spectrum of **1[PF$_6$]** in CH_3CN. *inset*: isotopic distribution of mass spectrum of **1[PF$_6$]** of experimentally obtained (black line), simulated (red line).

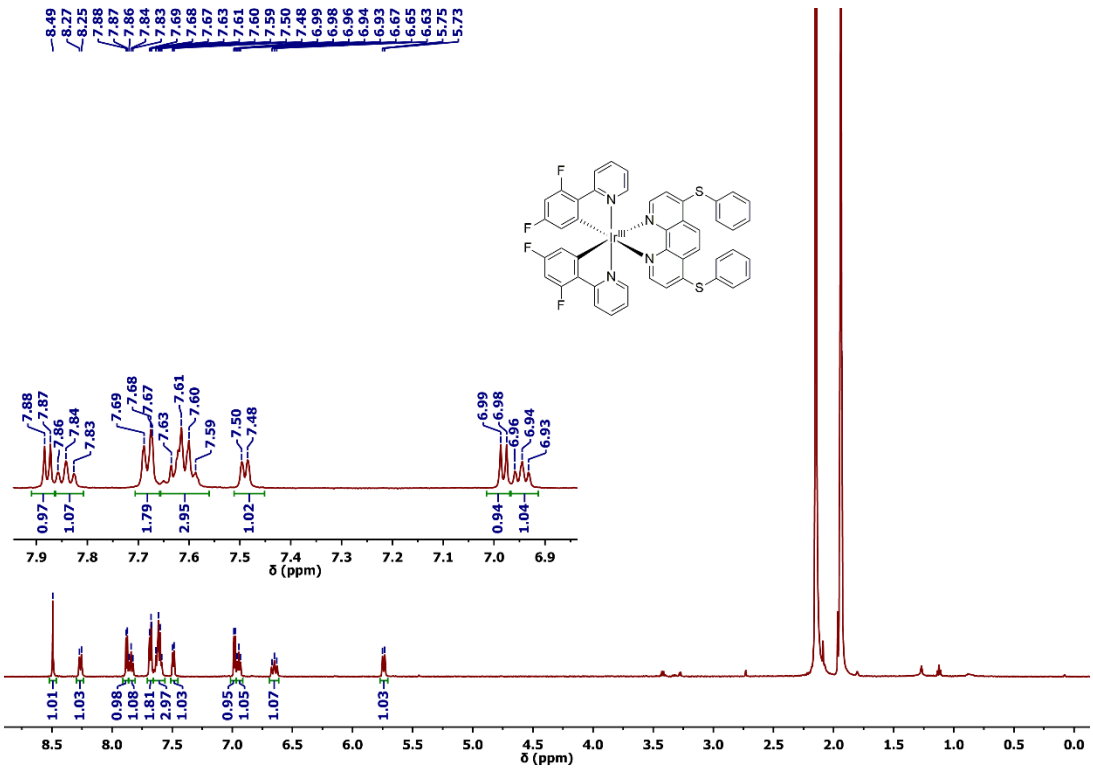

Fig. S8. ^{1}H NMR spectrum of **2[PF$_6$]** in CD_3CN.

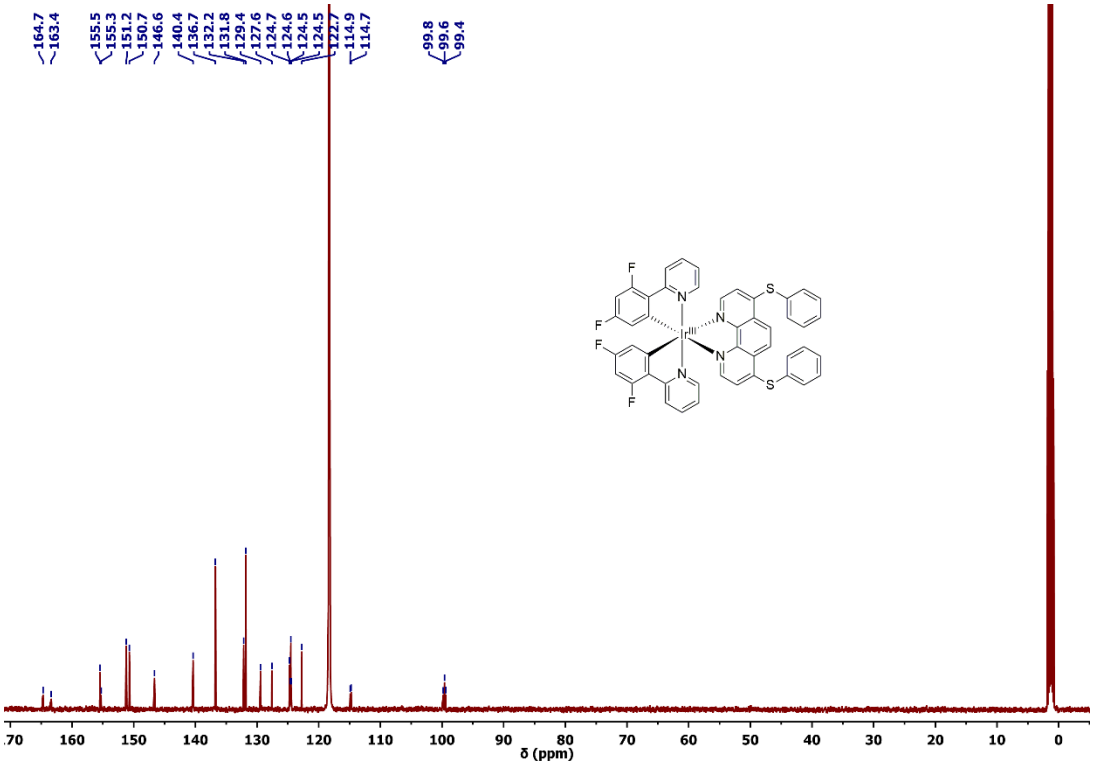

Fig. S9. ^{13}C NMR spectrum of **2[PF$_6$]** in CD_3CN.

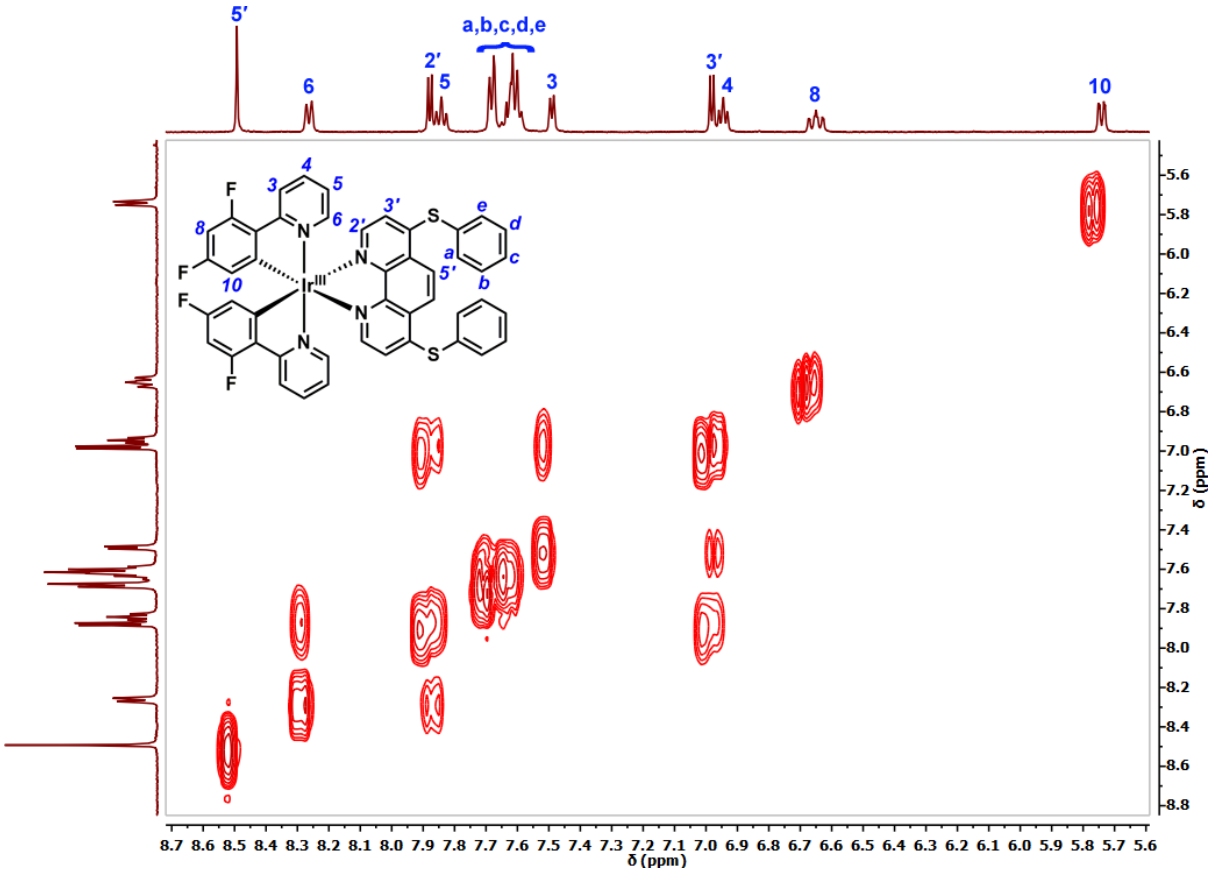

Fig. S10. Partial ^{1}H-^{1}HCOSY NMR spectrum of **2[PF$_6$]** in CD_3CN.

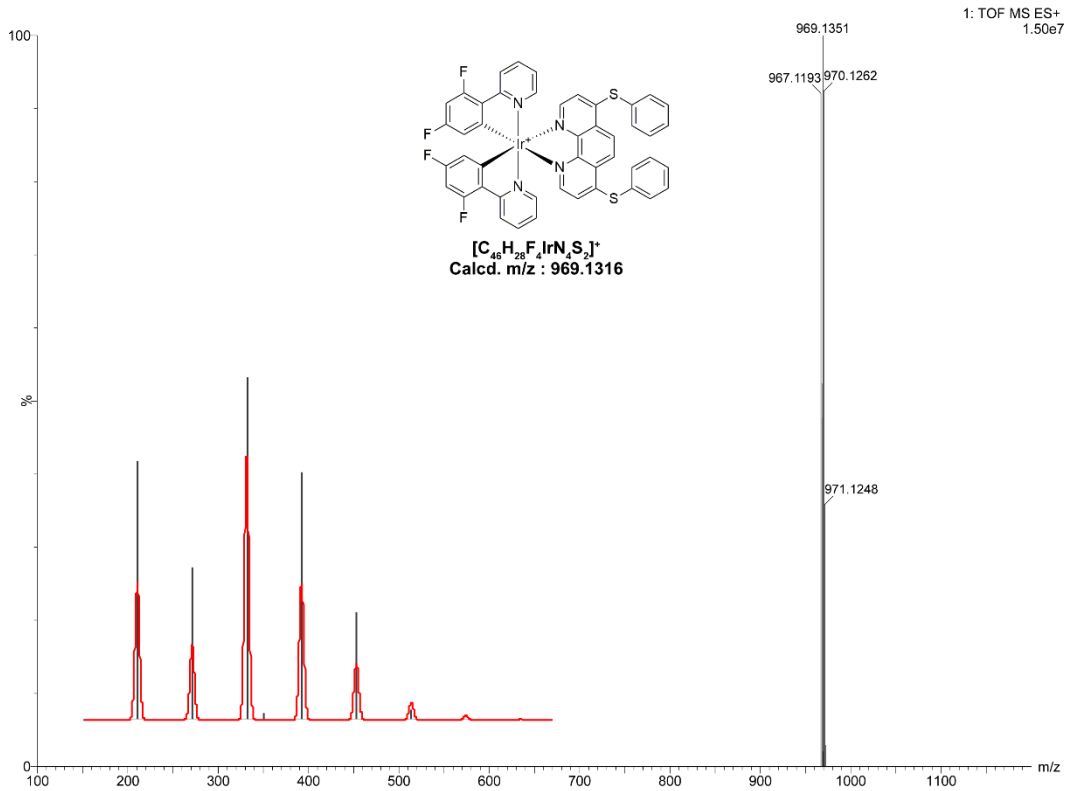

Fig. S11. HRMS spectrum of **2[PF$_6$]** in CH_3CN. *Inset*: isotopic distribution of mass spectrum of **2[PF$_6$]** of experimentally obtained (black line), simulated (red line).

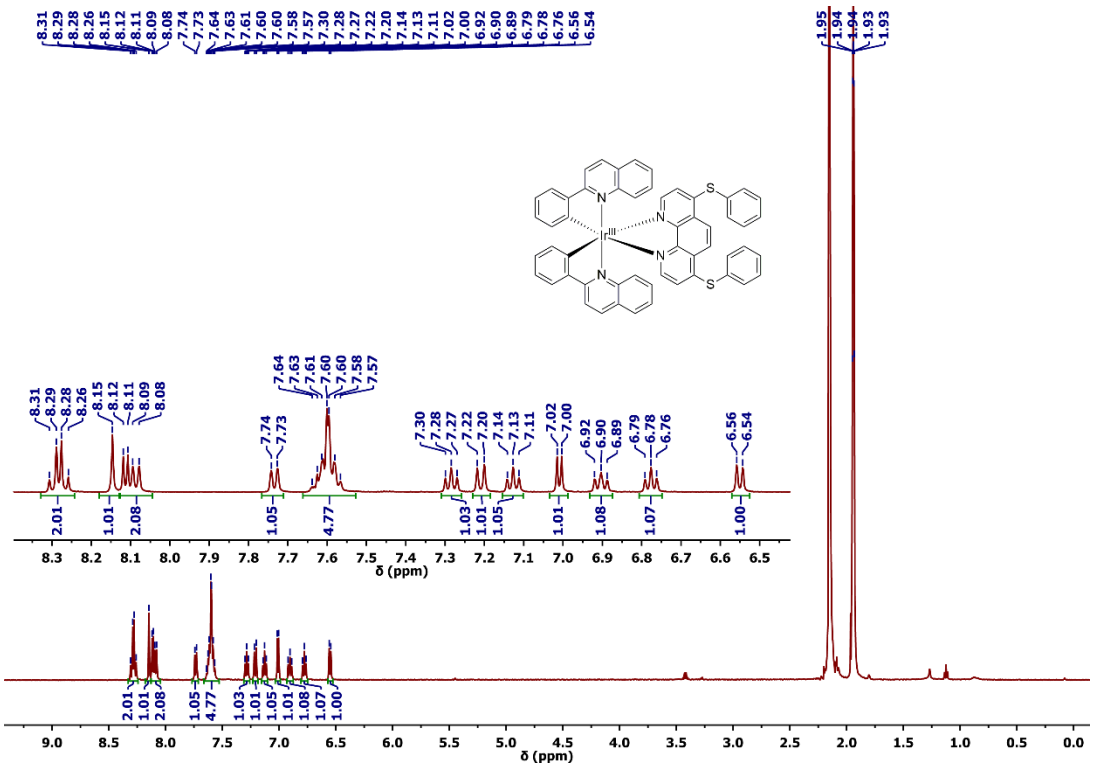

Fig. S12. ^{1}HNMR spectrum of **3[PF$_6$]** in CD_3CN.

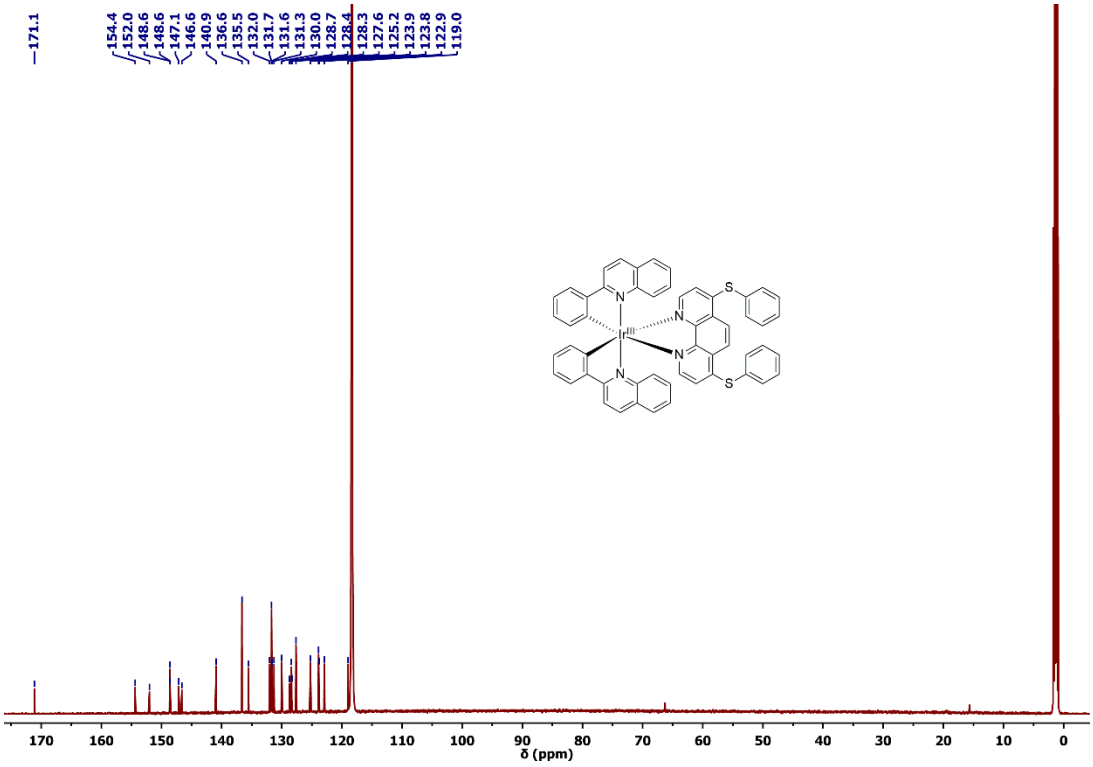

Fig. S13. ^{13}C NMR spectrum of **3[PF$_6$]** in CD_3CN.

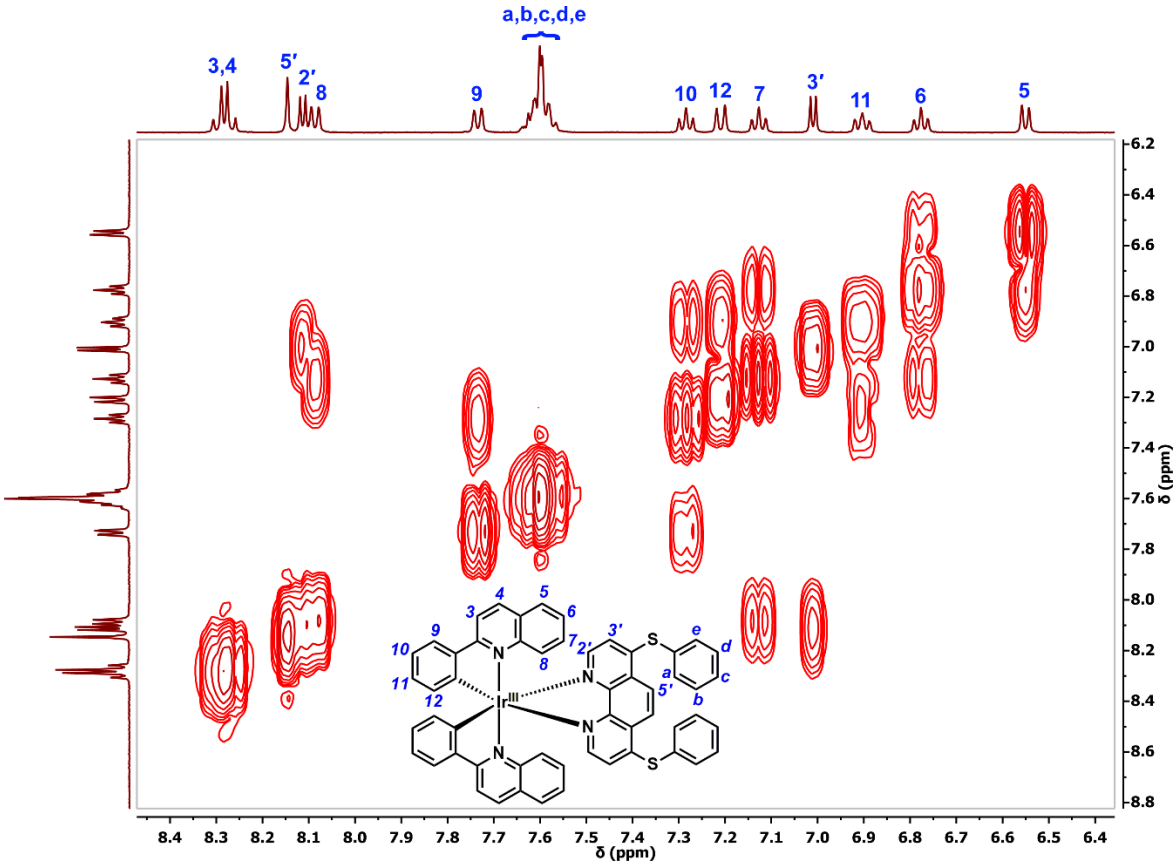

Fig. S14. Partial ^{1}H-^{1}HCOSY NMR spectrum of **3[PF$_6$]** in CD_3CN.

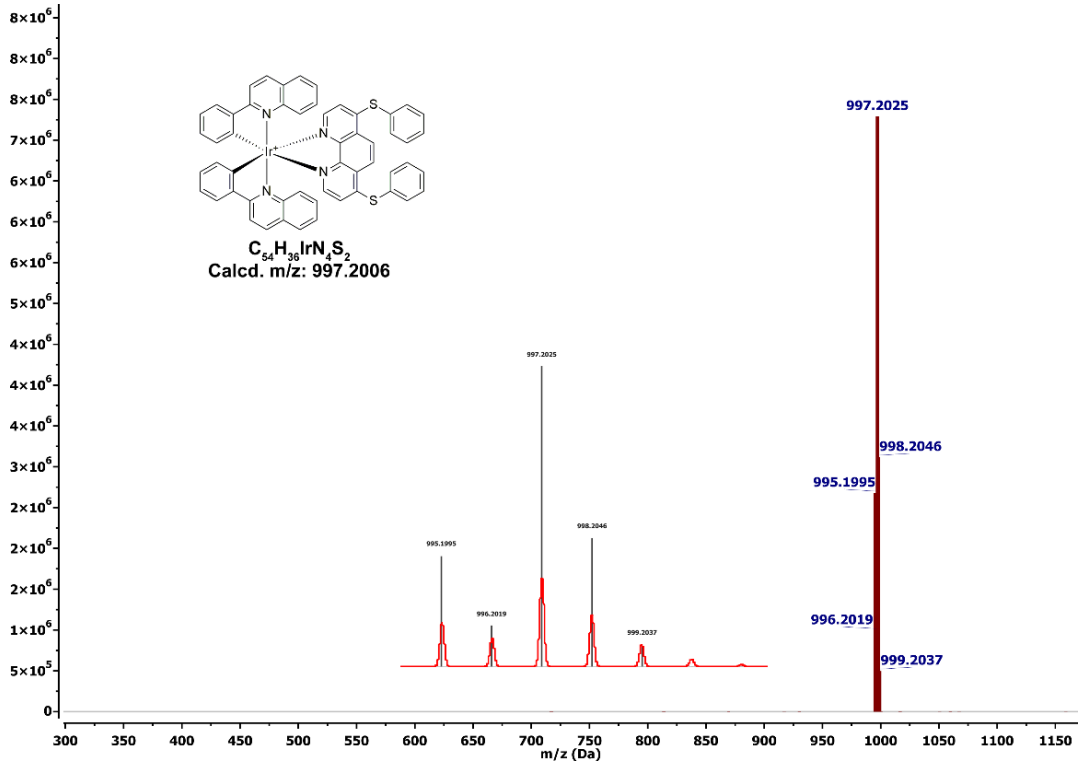

Fig. S15. HRMS spectrum of **3[PF6]** in CH_3CN. *Inset*: isotopic distribution of mass spectrum of **3[PF6]** of experimentally obtained (black line), simulated (red line).

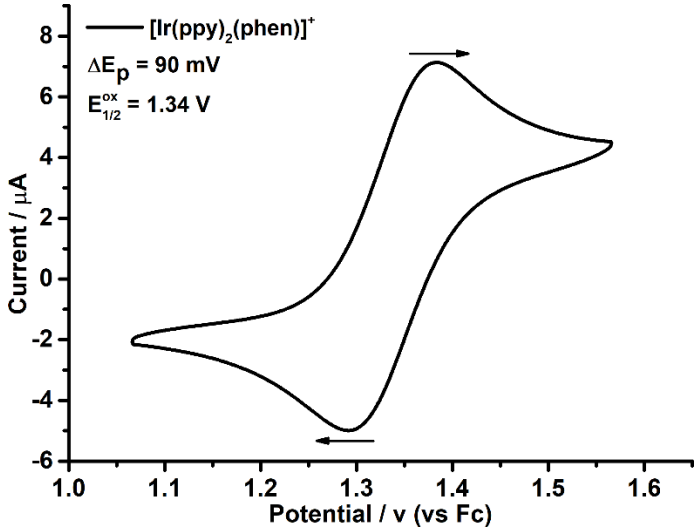

Fig. S16. Cyclic voltammogram of $[Ir(ppy)_2(phen)](PF_6)$, with 0.1 M Bu_4NClO_4 in dry and degassed CH_3CN versus the Fc/Fc^+ couple.

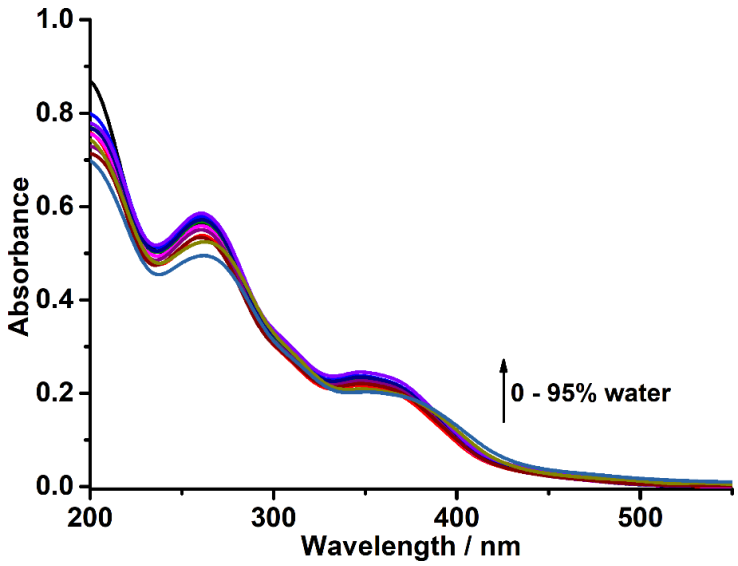

Fig. S17. UV-vis spectra of **1[PF$_6$]** in CH_3CN with different water (0-95%).

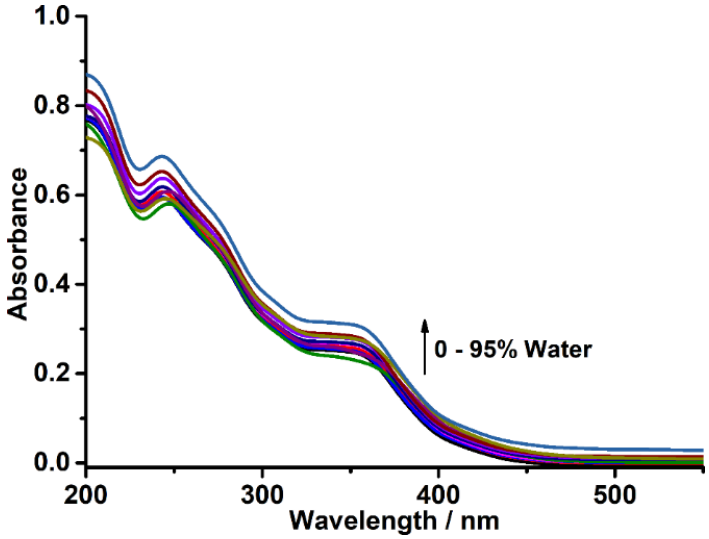

Fig. S18. UV-vis spectra of **2[PF$_6$]** in CH_3CN with different water (0-95%).

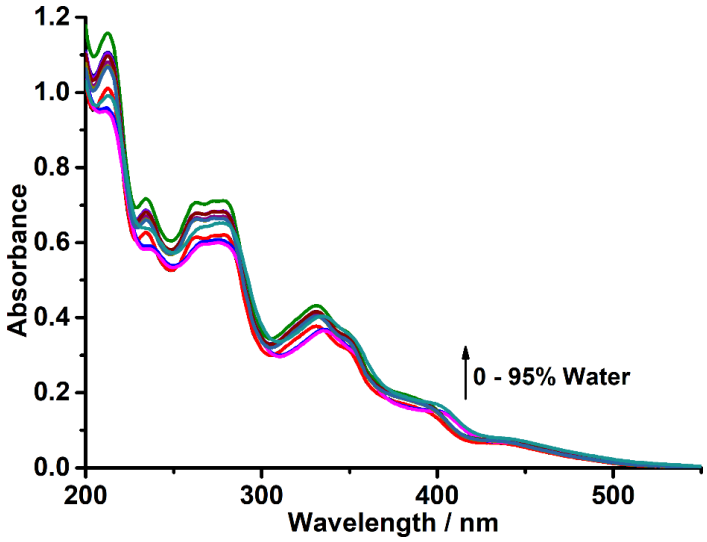

Fig. S19. UV-vis spectra of **3[PF$_6$]** in CH_3CN with different water (0-95%).

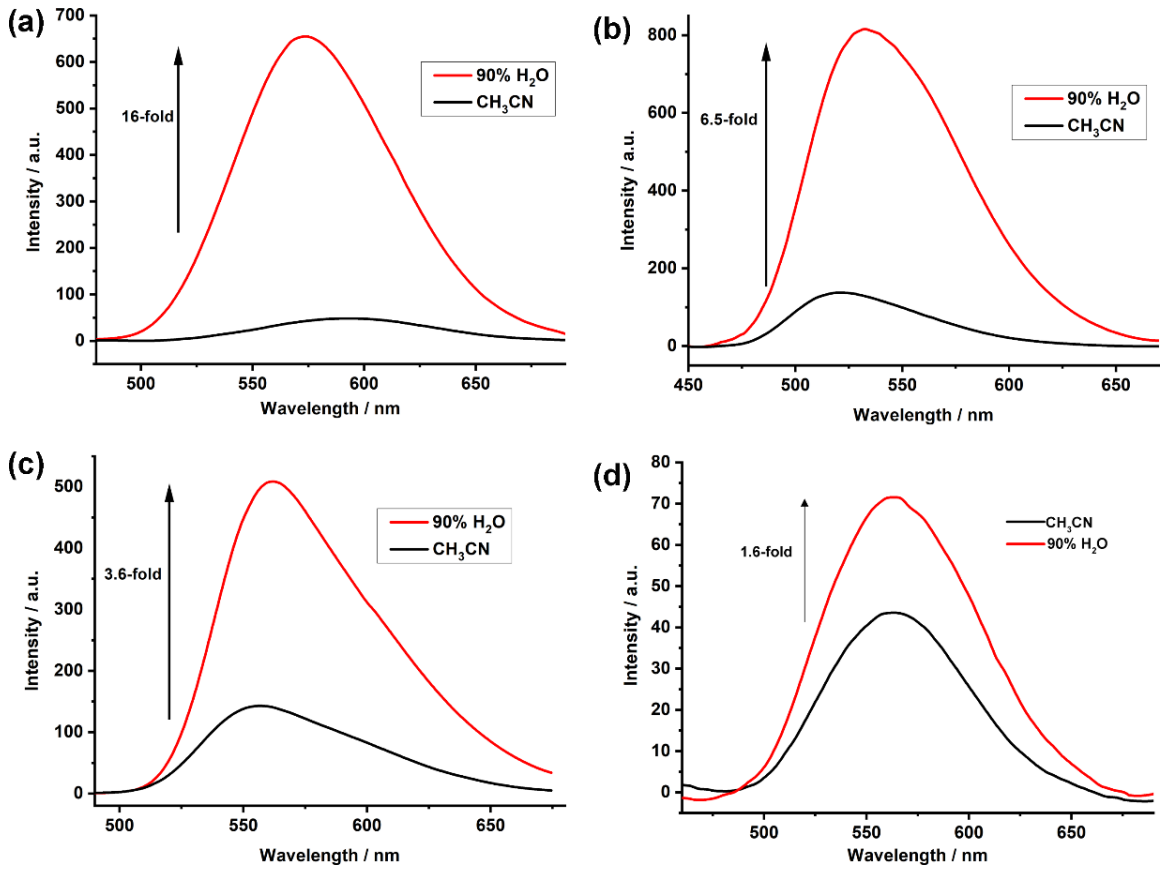

Fig. S20. PL spectra of compound (a) **1** (b) **2** (c) **3** and (d) $[Ir(ppy)_2(phen)]PF_6$ in CH_3CN and 90% water-CH_3CN mixture.

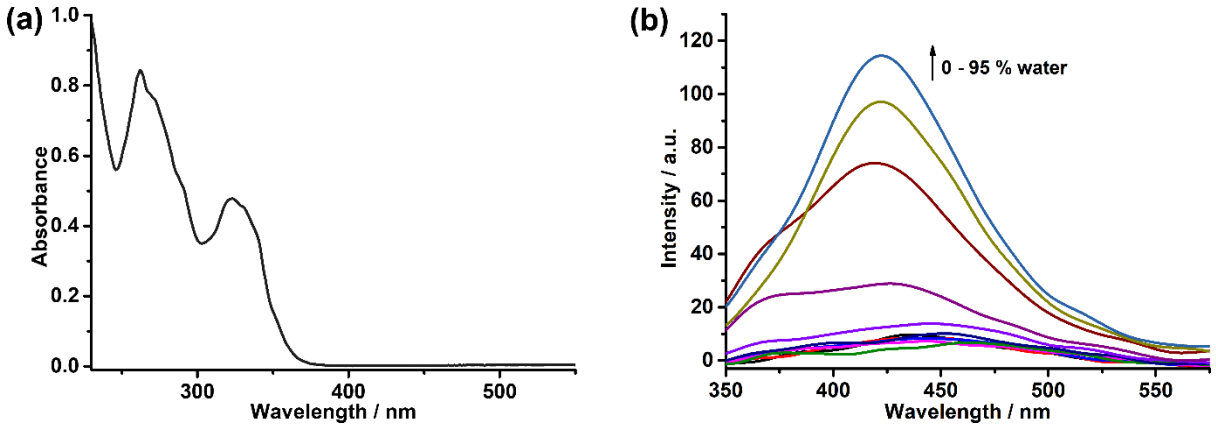

Fig. S21. (a) UV-vis spectrum of **L** (25 μM), and (b) PL spectrum of **L** in methanol with different water (0-95%).

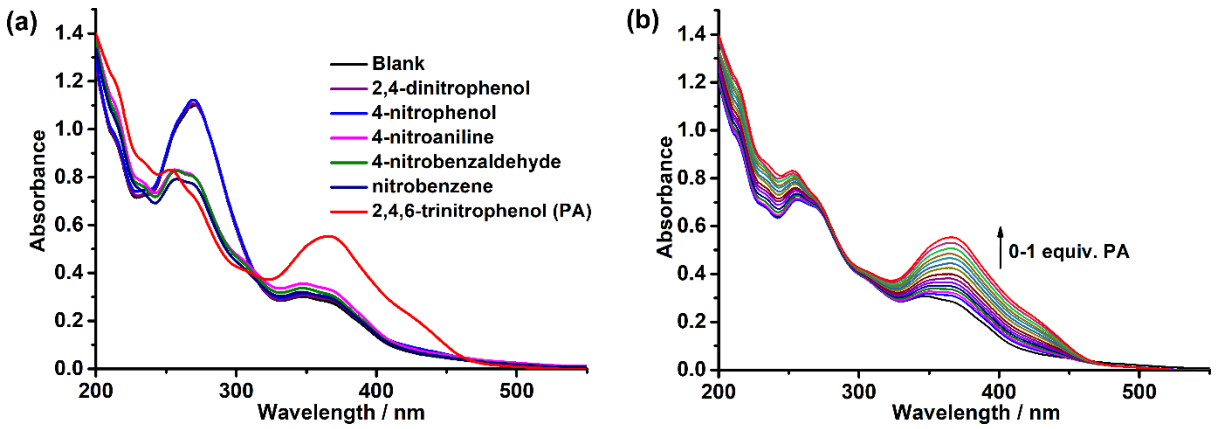

Fig. S22. (a) UV-vis selectivity of **1[PF$_6$]** (10 μM) in the presence of various NACs (10 μM) in 90% aqueous acetonitrile solution at room temperature, (b) UV-vis titration of **1[PF$_6$]** (10 μM) with PA (0-1 equiv.).

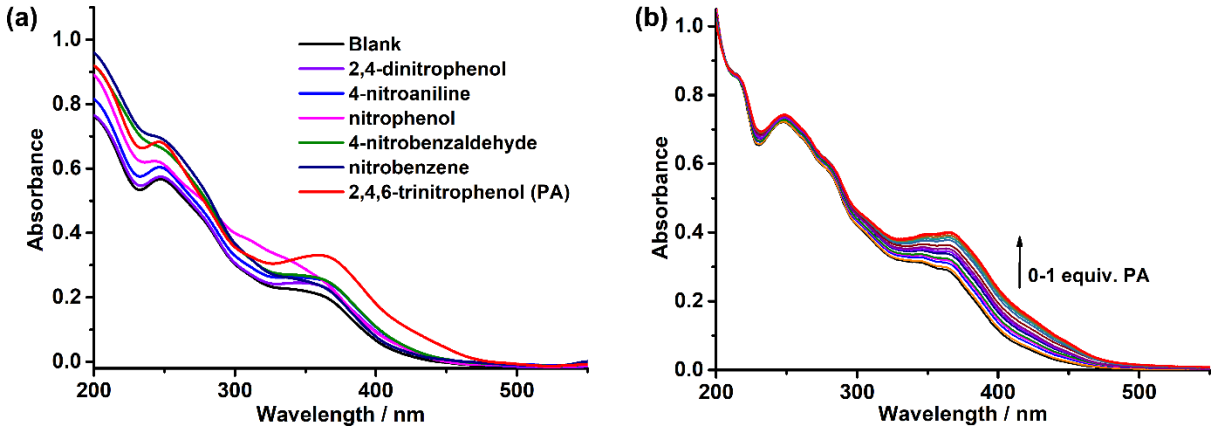

Fig. S23. (a) UV-vis selectivity of **2[PF$_6$]** (10 μM) in the presence of various NACs (10 μM) in 90% aqueous acetonitrile solution at room temperature, (b) UV-vis titration of **2[PF$_6$]** (10 μM) with PA (0-1 equiv.).

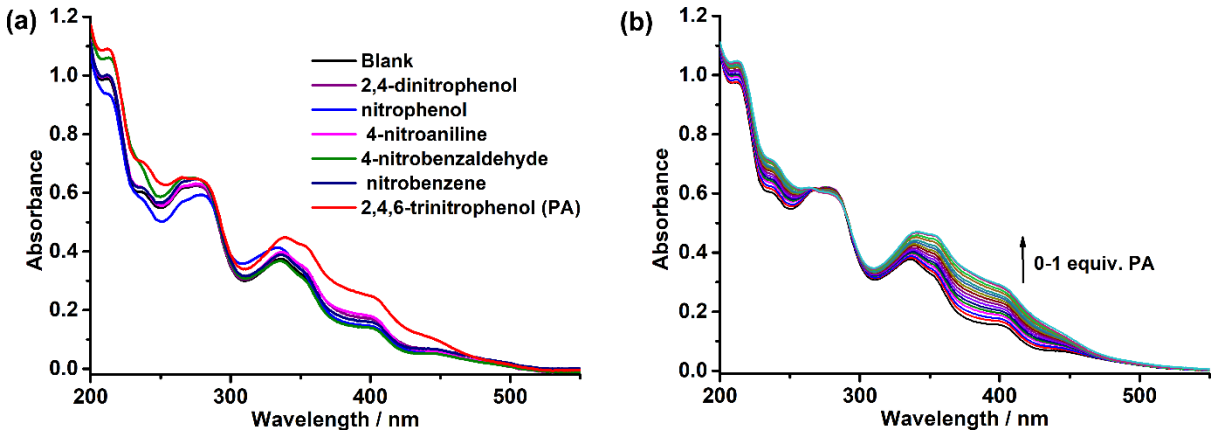

Fig. S24. (a) UV-vis selectivity of **3[PF$_6$]** (10 μM) in the presence of various NACs (10 μM) in 90% aqueous acetonitrile solution at room temperature, (b) UV-vis titration of **3[PF$_6$]** (10 μM) with PA (0-1 equiv.).

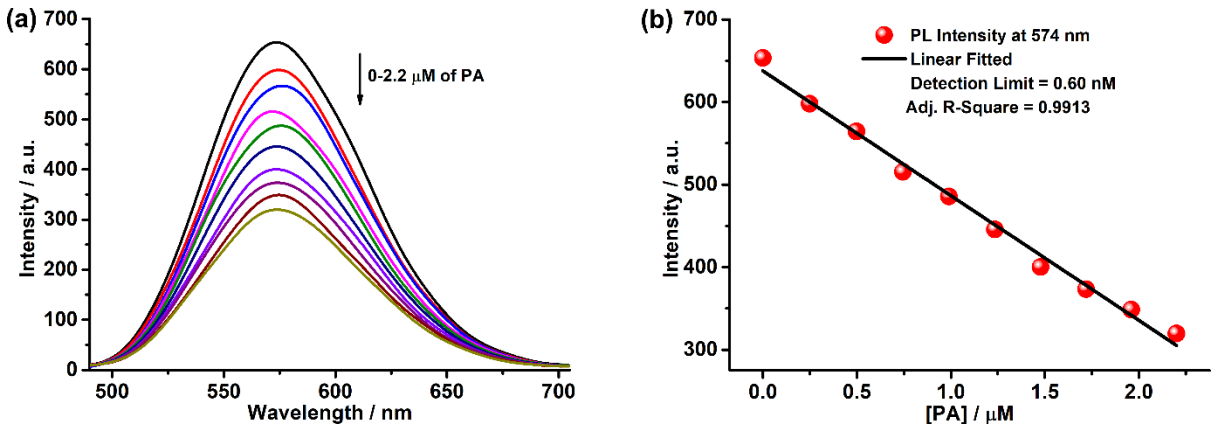

Fig. S25. (a) A PL titration of **1[PF$_6$]** (10 μM) with PA (0–2.2 μM) for the calculation of the limit of detection. (b) A calibration curve over a PA concentration ranges from 0–2.2 μM.

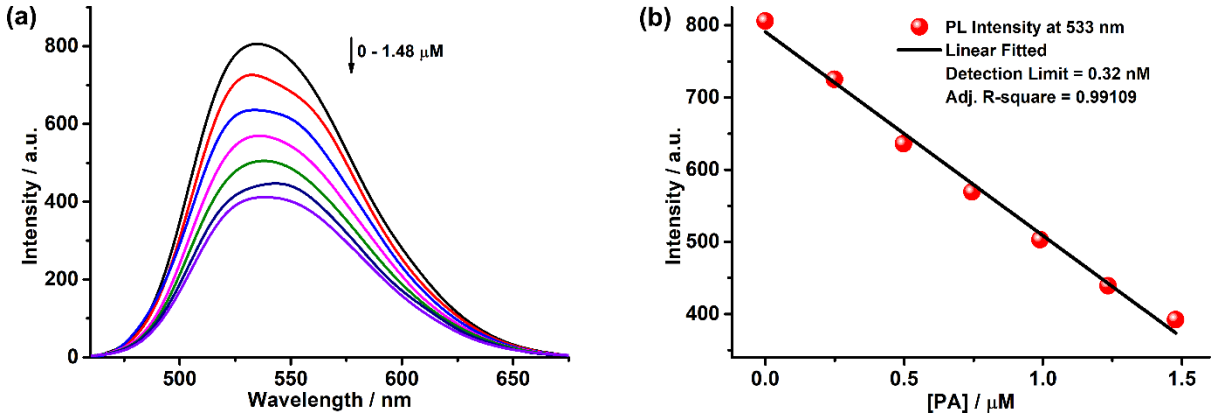

Fig. S26. (a) A PL titration of **2[PF$_6$]** (10 μM) with PA (0–1.48 μM) for the calculation of the limit of detection. (b) A calibration curve over a PA concentration ranges from 0–1.48 μM.

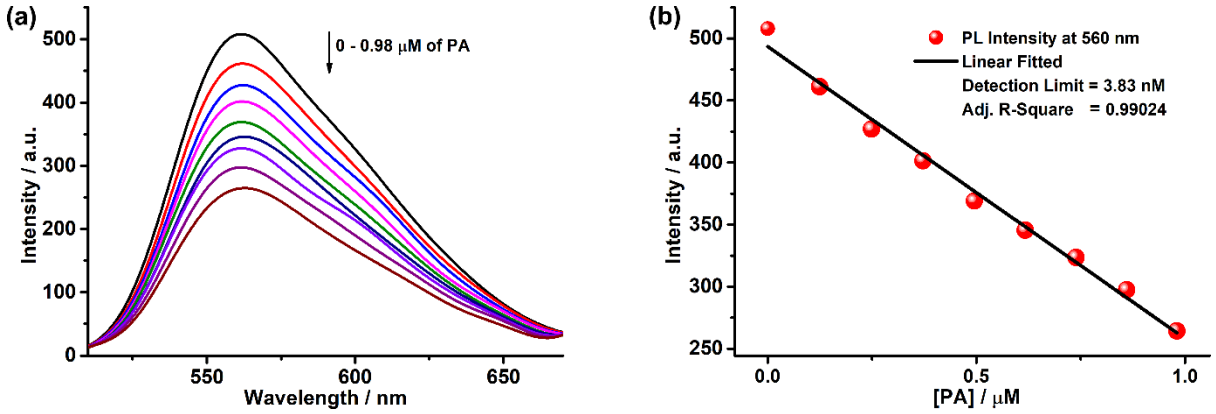

Fig. S27. (a) A PL titration of **3[PF$_6$]** (10 μM) with PA (0–0.98 μM) for the calculation of the limit of detection. (b) A calibration curve over a PA concentration ranges from 0–0.98 μM.

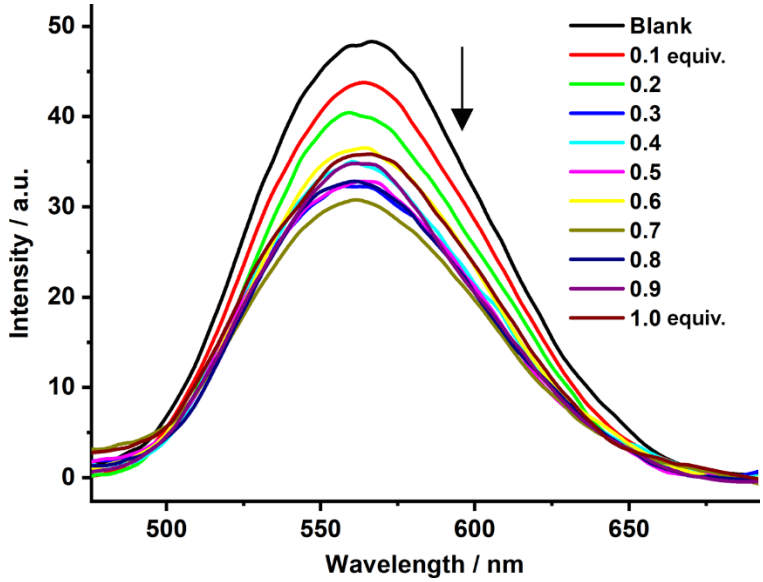

Fig. S28. PL titration of $[Ir(ppy)_2(phen)]PF_6$ (10 μM) with PA (0–10 μM) [λ_{ex} = 358 nm, λ_{em} = 562 nm].

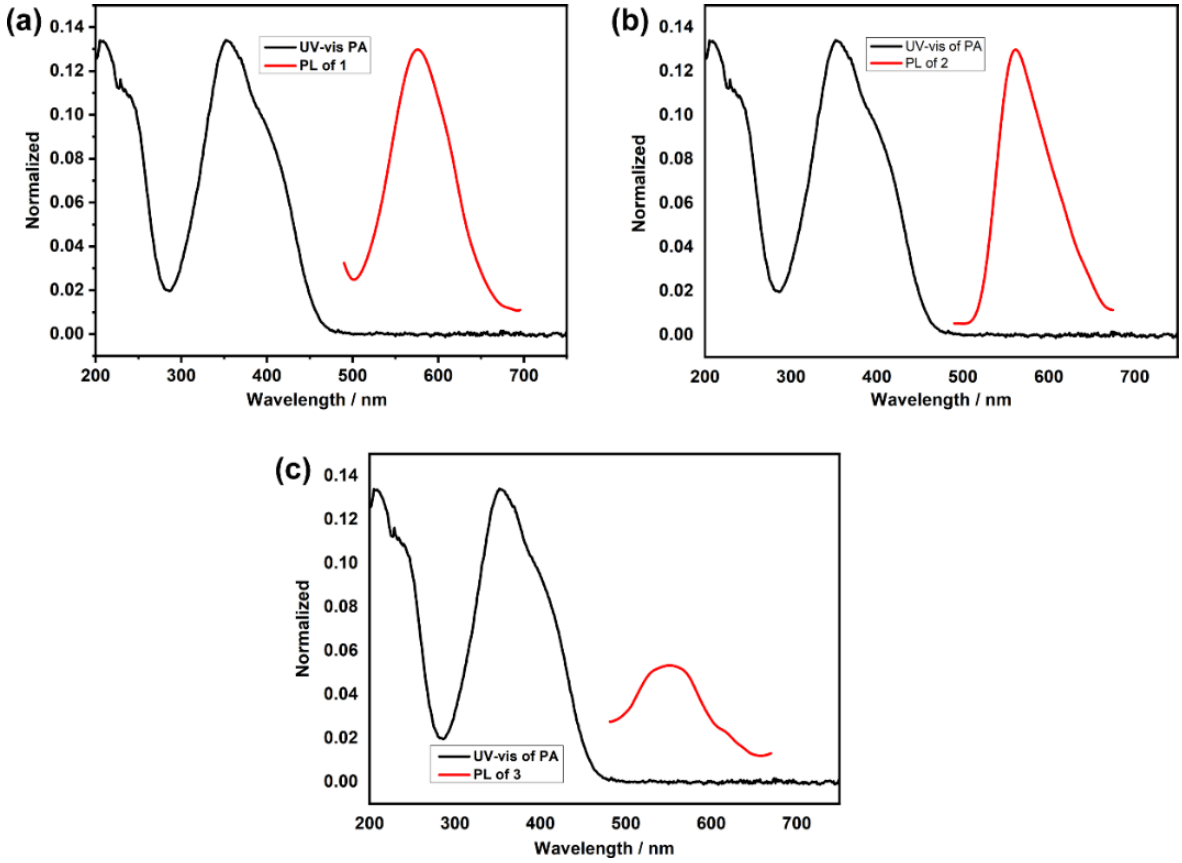

Fig. S29. Normalized UV−vis spectrum of PA and normalized emission spectrum of compound (a) **1** (b) **2** (c) **3** in 90% aqueous media.

Table S1. Crystal data and structure refinement for **1[PF_6]**.

Empirical formula	$C_{46}H_{32}F_6IrN_4PS_2$	
Formula weight	1042.04	
Temperature	293(2) K	
Wavelength	0.71073 Å	
Crystal system	Monoclinic	
Space group	*C*2/c	
Unit cell dimensions	a = 24.115(5) Å	α= 90°.
	b = 20.342(5) Å	β= 103.492(12)°.
	c = 17.437(4) Å	γ = 90°.
Volume	8318(3) $Å^3$	
Z	8	
Density (calculated)	1.664 Mg/m^3	
Absorption coefficient	3.415 mm^{-1}	
F(000)	4112	
Crystal size	0.160 x 0.150 x 0.080 mm^3	
Theta range for data collection	1.325 to 28.451°.	
Index ranges	-31<=h<=32, -27<=k<=27, -23<=l<=23	
Reflections collected	109257	
Independent reflections	10437 [*R*(int) = 0.0950]	
Completeness to theta = 25.242°	100.0 %	
Absorption correction	Semi-empirical from equivalents	
Max. and min. transmission	0.789 and 0.612	
Refinement method	Full-matrix least-squares on F^2	
Data / restraints / parameters	10437 / 0 / 542	
Goodness-of-fit on F^2	1.083	
Final R indices [*I>2sigma(I)*][a]	*R*1 = 0.0348, *wR*2 = 0.0935	
R indices (all data)[a]	*R*1 = 0.0555, *wR*2 = 0.1150	
Largest diff. peak and hole	0.728 and -1.397 e.$Å^{-3}$	

[a] $R1 = \Sigma||F_o| - |F_c||/\Sigma|F_o|$; $wR2 = \{\Sigma[w(F_o^2 - F_c^2)^2]/\Sigma w(F_o^2)^2\}^{1/2}$

Table S2. Selected bond lengths (Å) and angles (°) around the Ir(III) in complex **1[PF_6]**.

Bond lengths (Å)			
C(35)-Ir(1)	2.013(4)	C(46)-Ir(1)	2.013(4)
N(1)-Ir(1)	2.155(3)	N(2)-Ir(1)	2.151(3)
N(3)-Ir(1)	2.048(3)	N(4)-Ir(1)	2.051(3)
Bond angles (°)			
C(35)-Ir(1)-C(46)	90.69(16)	C(35)-Ir(1)-N(3)	80.07(15)
C(46)-Ir(1)-N(3)	96.60(16)	C(35)-Ir(1)-N(4)	98.09(15)
C(46)-Ir(1)-N(4)	79.92(16)	N(3)-Ir(1)-N(4)	176.07(13)
C(35)-Ir(1)-N(2)	172.98(14)	C(46)-Ir(1)-N(2)	96.05(15)
N(3)-Ir(1)-N(2)	97.18(13)	N(4)-Ir(1)-N(2)	85.04(13)
C(35)-Ir(1)-N(1)	96.48(14)	C(46)-Ir(1)-N(1)	172.82(14)
N(3)-Ir(1)-N(1)	84.94(13)	N(4)-Ir(1)-N(1)	98.74(14)
N(2)-Ir(1)-N(1)	76.79(12)		

Table S3. Crystal data and structure refinement for complex **2[PF$_6$]**.

Empirical formula	$C_{92}H_{56}F_{20}Ir_2N_8P_2S_4$	
Formula weight	2228.02	
Temperature	293(2) K	
Wavelength	0.71073 Å	
Crystal system	Triclinic	
Space group	*P* -1	
Unit cell dimensions	a = 13.6273(9) Å	α= 64.763(2)°.
	b = 18.5596(12) Å	β= 80.330(2)°.
	c = 19.5788(11) Å	γ = 80.923(2)°.
Volume	4394.9(5) Å^3	
Z	2	
Density (calculated)	1.684 Mg/m^3	
Absorption coefficient	3.250 mm^{-1}	
F(000)	2184	
Crystal size	0.720 x 0.210 x 0.180 mm^3	
Theta range for data collection	1.996 to 28.370°.	
Index ranges	-18<=h<=18, -24<=k<=24, -26<=l<=26	
Reflections collected	165890	
Independent reflections	21908 [R(int) = 0.0608]	
Completeness to theta = 25.242°	99.9 %	
Absorption correction	Semi-empirical from equivalents	
Max. and min. transmission	0.592 and 0.203	
Refinement method	Full-matrix least-squares on F^2	
Data / restraints / parameters	21908 / 0 / 1153	
Goodness-of-fit on F^2	1.133	
Final R indices [*I>2sigma(I)*][a]	*R1* = 0.0436, *wR2* = 0.0933	
R indices (all data)[a]	*R1* = 0.0618, *wR2* = 0.1056	
Largest diff. peak and hole	2.295 and -1.117 e.Å^{-3}	

[a] $R1 = \Sigma||F_o| - |F_c||/\Sigma|F_o|$; $wR2 = \{\Sigma[w(F_o^2 - F_c^2)^2]/\Sigma w(F_o^2)^2\}^{1/2}$

Table S4. Selected bond lengths (Å) and angles (°) around the Ir(III) in complex **2[PF_6]**.

	Bond lengths (Å)		
C(35)-Ir(1)	2.004(6)	C(46)-Ir(1)	1.998(6)
N(1)-Ir(1)	2.135(4)	N(2)-Ir(1)	2.140(4)
N(3)-Ir(1)	2.043(4)	N(4)-Ir(1)	2.044(4)
C(81)-Ir(2)	2.012(4)	C(92)-Ir(2)	2.009(4)
N(5)-Ir(2)	2.137(3)	N(6)-Ir(2)	2.136(4)
N(7)-Ir(2)	2.035(4)	N(8)-Ir(2)	2.047(4)
	Bond angles (°)		
C(46)-Ir(1)-C(35)	93.3(2)	C(46)-Ir(1)-N(3)	96.7(2)
C(35)-Ir(1)-N(3)	80.5(2)	C(46)-Ir(1)-N(4)	80.3(2)
C(35)-Ir(1)-N(4)	93.3(2)	N(3)-Ir(1)-N(4)	172.96(17)
C(46)-Ir(1)-N(1)	171.3(2)	C(35)-Ir(1)-N(1)	95.22(19)
N(3)-Ir(1)-N(1)	86.47(15)	N(4)-Ir(1)-N(1)	97.40(16)
C(46)-Ir(1)-N(2)	94.1(2)	C(35)-Ir(1)-N(2)	172.3(2)
N(3)-Ir(1)-N(2)	96.64(17)	N(4)-Ir(1)-N(2)	89.96(17)
N(1)-Ir(1)-N(2)	77.43(15)	C(92)-Ir(2)-C(81)	89.19(16)
C(92)-Ir(2)-N(7)	93.01(18)	C(81)-Ir(2)-N(7)	80.54(18)
C(92)-Ir(2)-N(8)	80.36(19)	C(81)-Ir(2)-N(8)	95.11(19)
N(7)-Ir(2)-N(8)	172.17(15)	C(92)-Ir(2)-N(6)	97.33(15)
C(81)-Ir(2)-N(6)	173.31(15)	N(7)-Ir(2)-N(6)	97.57(15)
N(8)-Ir(2)-N(6)	87.47(16)	C(92)-Ir(2)-N(5)	174.29(15)
C(81)-Ir(2)-N(5)	96.42(15)	N(7)-Ir(2)-N(5)	88.93(15)
N(8)-Ir(2)-N(5)	98.06(16)	N(6)-Ir(2)-N(5)	77.08(13)

Table S5. Crystal data and structure refinement for complex **3[PF$_6$]•CH$_2$Cl$_2$**.

Empirical formula	$C_{55}H_{38}Cl_2F_6IrN_4PS_2$	
Formula weight	1227.08	
Temperature	293(2) K	
Wavelength	0.71073 Å	
Crystal system	Monoclinic	
Space group	*P* 21/n	
Unit cell dimensions	a = 11.5156(6) Å	α= 90°.
	b = 15.6986(8) Å	β= 100.737(2)°.
	c = 27.5367(13) Å	γ = 90°.
Volume	4890.9(4) Å^3	
Z	4	
Density (calculated)	1.666 Mg/m^3	
Absorption coefficient	3.024 mm^{-1}	
F(000)	2432	
Crystal size	0.180 x 0.120 x 0.100 mm^3	
Theta range for data collection	1.500 to 28.522°.	
Index ranges	-15<=h<=15, -20<=k<=20, -36<=l<=36	
Reflections collected	50197	
Independent reflections	12252 [R(int) = 0.0680]	
Completeness to theta = 25.242°	99.9 %	
Absorption correction	Semi-empirical from equivalents	
Max. and min. transmission	0.746 and 0.343	
Refinement method	Full-matrix least-squares on F^2	
Data / restraints / parameters	12252 / 0 / 640	
Goodness-of-fit on F^2	1.064	
Final R indices [*I>2sigma(I)*][a]	R1 = 0.0433, wR2 = 0.1030	
R indices (all data)[a]	R1 = 0.0743, wR2 = 0.1240	
Largest diff. peak and hole	0.892 and -0.931 e.Å^{-3}	

[a] $R1 = \Sigma||F_o| - |F_c||/\Sigma|F_o|$; $wR2 = \{\Sigma[w(F_o^2 - F_c^2)^2]/\Sigma w(F_o^2)^2\}^{1/2}$.

Table S6. Selected bond lengths (Å) and angles (°) around the Ir(III) in complex **3[PF_6]•CH_2Cl_2**.

Bond lengths (Å)			
C(39)-Ir(1)	2.002(5)	C(54)-Ir(1)	1.996(5)
N(1)-Ir(1)	2.154(4)	N(2)-Ir(1)	2.206(4)
N(3)-Ir(1)	2.087(4)	N(4)-Ir(1)	2.084(4)
Bond angles (°)			
C(54)-Ir(1)-C(39)	91.8(2)	C(54)-Ir(1)-N(4)	79.91(18)
C(39)-Ir(1)-N(4)	94.16(18)	C(54)-Ir(1)-N(3)	94.36(18)
C(39)-Ir(1)-N(3)	79.90(19)	N(4)-Ir(1)-N(3)	171.68(14)
C(54)-Ir(1)-N(1)	170.71(16)	C(39)-Ir(1)-N(1)	97.32(17)
N(4)-Ir(1)-N(1)	100.85(15)	N(3)-Ir(1)-N(1)	85.78(14)
C(54)-Ir(1)-N(2)	96.18(17)	C(39)-Ir(1)-N(2)	167.99(18)
N(4)-Ir(1)-N(2)	78.52(14)	N(3)-Ir(1)-N(2)	108.28(14)
N(1)-Ir(1)-N(2)	75.02(14)		

Calculation of Limit of Detection

The detection limit was calculated based on PL titration data. To determine the S/N ratio, the standard deviation of the blank solution was calculated with ten replicate data of the complexes in PL spectroscopy. Finally, the limit of detection (LOD) of **1[PF$_6$]**, **2[PF$_6$]**, and **3[PF$_6$]** for picric acid was determined from the following equation.

$$LOD = 3\sigma/K$$

Here σ is the standard deviation of the blank solution, and K is the slope obtained from the plot of the calibration curve.

Calculation of Quantum Yield

The quantum yields of **1[PF$_6$]**, **2[PF$_6$]**, and **3[PF$_6$]** were determined in dry and deaerated CH_3CN. $[Ru(bpy)_3](PF_6)_2$ (Φ_R = 0.062 in acetonitrile) for **1[PF$_6$]** and **3[PF$_6$]**; Quinine sulfate (Φ_R = 0.60 in 0.5 M H_2SO_4) for **2[PF$_6$]** were used as a references.[1] The quantum yield is calculated according to the following equation:

$$\Phi_S = \Phi_R \times \frac{1 - 10^{-A_R}}{1 - 10^{-A_S}} \times \frac{I_S}{I_R} \times \frac{{\eta_S}^2}{{\eta_R}^2}$$

Where S and R indicate the unknown and standard solutions, respectively, Φ is the quantum yield, I is the integrated area under the emission spectra, A is the absorbance, and η is the refractive index of the solvent.

Electrochemistry

A three electrodes cell system was taken for electrochemical analysis. The setup contains a Pt working electrode, a Pt wire auxiliary electrode, and an Ag wire as a pseudo-reference electrode. Experiments were performed on 1.0 mM dry and degassed (N_2) acetonitrile solution of **1[PF$_6$]**, **2[PF$_6$]**, and **3[PF$_6$]** in the presence of supporting electrolyte tetra-n-butylammonium

perchlorate (0.10 M). To compare the oxidation potential of these complexes, the cyclic voltammetry data of $[Ir(ppy)_2phen]^+$ was also collected under the same experimental conditions. The electrochemical potential window was calibrated using ferrocene (as the internal standard) after each experiment. The standard redox potential of the ferrocene/ferrocenium (Fc/Fc^+) couple was taken as +0.400 V vs. Ag wire electrode.[2] A scan rate of 100 mV s^{-1} was fixed for all the measurements.

Calculation of Excited States Lifetimes

The luminescence lifetimes of **1[PF$_6$], 2[PF$_6$] and 3[PF$_6$]** (10 μM) in the absence and presence of PA (1 equiv.) in acetonitrile and 90% aqueous media, were measured using TCSPC based fluorescence lifetime detection unit (PM-3) supplied by PTI. The sample was excited by 374 nm laser diode supplied by PTI. The fluorescence decays were monitored at the corresponding emission maxima as observed in the steady-state fluorescence measurement. The collected fluorescence decay traces from the sample were analyzed by non-linear least square analysis based on the Levenberg–Marquardt algorithm with reference to the instrument response function (IRF), collected at the excitation wavelength using a scattering solution. Validity of the fitting analysis was investigated by various statistical parameters like the Durbin-Watson (DW) and reduced chi-squared (χ^2) parameter values and visually observing the distribution of weighted residuals. The fluorescence decay was found to be both single exponential and double exponential fitting model to adequately describe the obtained decay traces. Average lifetimes ($<\tau>$) were calculated using the following decay equation

$$<\tau> = \sum \alpha_i \tau_i$$

Whereas, α_i is the amplitude of the ith decay component ($\alpha_i = \alpha_i/\Sigma\alpha_i$) and τ_i is the excited state luminescence lifetime of the ith component.

Table S7: TCSPS Data for the fluorescene lifetime calculation

Compound	τ_1	τ_2	α_1	α_2	τ_{av}
1[PF_6] (single exponential)	112	0	100	0	112 ns
1[PF_6] +PA	56.81	7.026	63.47	36.53	53.5 ns
2[PF_6] (single exponential)	138	0	100	0	138 ns
2[PF_6] +PA	0.33	11.6	99.76	0.24	1.21 ns
3[PF_6] (single exponential)	140	0	100	0	140 ns
3[PF_6] +PA	51.52	5.925	64.94	35.06	48.85 ns

Computational Studies

The geometry optimization of complex **1**, **2**, **3** and Picric acid (singlet) was performed with the Gaussian 09 and Gaussian 16 program packages using density functional theory (DFT). The B3LYP/6-31G(d,p)[3] basis set was used for C, H, N, F, and S, together with the LANL2DZ[4] for iridium. Time-dependent density functional theory (TDDFT) calculations at the ground-state geometry in acetonitrile were performed in conjunction with the conductor-like polarizable continuum model (CPCM)[5] for acetonitrile with a spin-restricted formalism to examine low-energy excitations at the same level of calculation. The triplet states TDDFT calculations were performed using the optimized ground state geometries at the same level as used in singlet state optimizations, along with CPCM for acetonitrile. A spin-unrestricted formalism was employed for singlet-triplet transitions in triplet states TDDFT calculations to study the nature of the non-emissive and emissive states of complex **1**, **2**, and **3**, respectively.

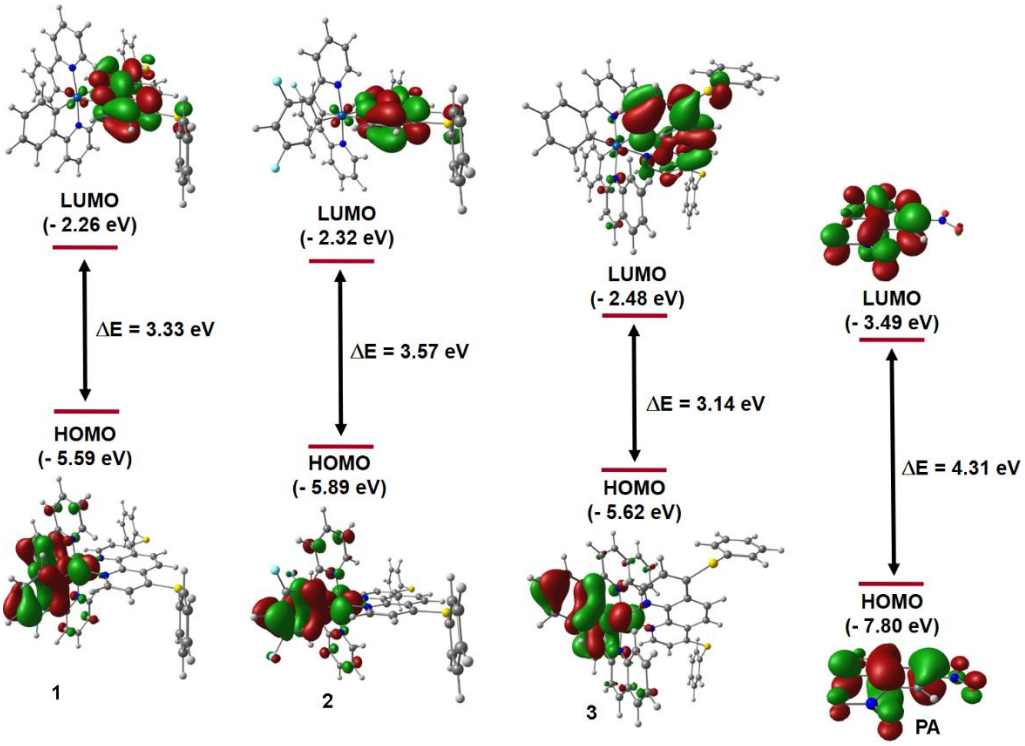

Fig. S30: Frontiers orbitals (HOMO and LUMO) of compounds **1**, **2**, **3** and PA for PET demonstration from compounds LUMO to the LUMO of PA.

Table S8: Excited states, their energies and oscillator strengths of compound **1[PF$_6$]**, **2[PF$_6$]** and **3[PF$_6$]**

1[PF$_6$]

Excited State 21: 3.015-A 1.8250 eV 679.36 nm f=0.0000 <S**2>=2.022
177B ->192B 0.10752
183B ->192B 0.99290

Excited State 22: 3.015-A 1.9029 eV 651.54 nm f=0.0002 <S**2>=2.023
181B ->192B 0.98489
182B ->192B -0.10838

Excited State 23: 3.015-A 1.9035 eV 651.35 nm f=0.0000 <S**2>=2.023
180B ->192B -0.11979
181B ->192B 0.10835
182B ->192B 0.98582

Excited State 24: 3.012-A 1.9407 eV 638.85 nm f=0.0003 <S**2>=2.018
193A ->202A -0.45237
193A ->205A 0.88971

Excited State 25: 3.014-A 1.9536 eV 634.64 nm f=0.0208 <S**2>=2.021
193A ->208A 0.13471
178B ->192B 0.90260
184B ->192B 0.32515

Excited State 26: 3.018-A 2.0357 eV 609.05 nm f=0.0018 <S**2>=2.026
193A ->204A 0.99810

Excited State 27: 3.017-A 2.0705 eV 598.80 nm f=0.0005 <S2>=2.026**
193A ->203A 0.46320 HOMO→LUMO+9
193A ->206A 0.88464 HOMO→LUMO+12

Excited State 28: 3.013-A 2.1451 eV 577.98 nm f=0.0040 <S**2>=2.020
174B ->192B 0.22304
176B ->192B 0.30048
177B ->192B 0.89983
183B ->192B -0.11480

Excited State 29: 3.023-A 2.1586 eV 574.37 nm f=0.1781 <S**2>=2.034
193A ->208A 0.87151
193A ->209A 0.40236
178B ->192B -0.15447
191B ->195B -0.14351

Excited State 30: 3.014-A 2.2659 eV 547.19 nm f=0.0003 <S**2>=2.021
193A ->201A -0.23286
193A ->207A 0.96447

Excited State 31: 3.017-A 2.4262 eV 511.03 nm f=0.0327 <S**2>=2.026
174B ->192B 0.33173
176B ->192B 0.83430
177B ->192B -0.36990

Excited State 32: 3.014-A 2.5814 eV 480.30 nm f=0.0004 <S**2>=2.021
193A ->208A -0.42074
193A ->209A 0.90472

Excited State 33: 3.014-A 2.7023 eV 458.80 nm f=0.0008 <S**2>=2.021
193A ->210A 0.97899
174B ->192B -0.15400

Excited State 34: 3.032-A 2.7365 eV 453.08 nm f=0.0311 <S**2>=2.048
193A ->210A 0.17029
174B ->192B 0.87598
176B ->192B -0.40389

Excited State 35: 3.039-A 2.7622 eV 448.85 nm f=0.0137 <S**2>=2.059
173B ->192B -0.20236
175B ->192B 0.96155

2[PF_6]

Excited State 18: 3.012-A 1.8332 eV 676.32 nm f=0.0149 <S**2>=2.018
209A ->213A 0.52645
209A ->214A 0.35021
209A ->216A 0.74158
209A ->221A -0.11320

Excited State 19: 3.010-A 1.8412 eV 673.40 nm f=0.0001 <S**2>=2.014
209A ->215A 0.98512

Excited State 20: 3.011-A 1.8641 eV 665.10 nm f=0.0016 <S**2>=2.016
209A ->213A -0.19629
209A ->214A 0.93500
209A ->216A -0.28052

Excited State 21: 3.009-A 1.9572 eV 633.47 nm f=0.0050 <S**2>=2.014
190B ->208B -0.13340
192B ->208B 0.10464
194B ->208B 0.95999

Excited State 22: 3.013-A 2.1431 eV 578.54 nm f=0.0000 <S**2>=2.019
209A ->217A 0.99553

Excited State 23: 3.031-A 2.2952 eV 540.19 nm f=0.2024 <S2>=2.047**
209A ->216A 0.12257 HOMO→LUMO+6
209A ->218A 0.16128 HOMO→LUMO+8
209A ->219A -0.18640
209A ->221A 0.85494 HOMO→LUMO+11
209A ->222A 0.15586 HOMO→LUMO+12
185B ->208B 0.10080
187B ->208B -0.15018
189B ->208B 0.14899
195B ->208B -0.12537
201B ->208B -0.12345
205B ->208B 0.10035

Excited State 24: 3.011-A 2.3061 eV 537.63 nm f=0.0024 <S**2>=2.017
190B ->208B -0.29395
192B ->208B 0.62812
193B ->208B 0.69466
194B ->208B -0.10490

Excited State 25: 3.012-A 2.3478 eV 528.08 nm f=0.0005 <S**2>=2.018
190B ->208B 0.56340
192B ->208B -0.45346
193B ->208B 0.66452
194B ->208B 0.13957

Excited State 26: 3.011-A 2.4704 eV 501.87 nm f=0.0005 <S**2>=2.016
209A ->218A 0.93758
209A ->219A -0.25275
209A ->221A -0.21385

Excited State 27: 3.013-A 2.5695 eV 482.52 nm f=0.0007 <S**2>=2.019
190B ->208B 0.56223
191B ->208B 0.63464
192B ->208B 0.47899
193B ->208B -0.17255

Excited State 28: 3.012-A 2.5969 eV 477.42 nm f=0.0020 <S**2>=2.018
190B ->208B -0.48498
191B ->208B 0.76380
192B ->208B -0.37489
193B ->208B 0.16613

Excited State 29: 3.011-A 2.6145 eV 474.22 nm f=0.0004 <S**2>=2.016
209A ->220A 0.90735
209A ->222A 0.34826
209A ->223A 0.11164
209A ->224A -0.15463

Excited State 30: 3.016-A 2.6792 eV 462.76 nm f=0.0037 <S**2>=2.024
209A ->216A 0.11811
209A ->218A 0.28529
209A ->219A 0.92336
209A ->221A 0.13973

Excited State 31: 3.014-A 2.6936 eV 460.29 nm f=0.0009 <S**2>=2.020
209A ->220A -0.34368
209A ->221A -0.17415
209A ->222A 0.77038
209A ->223A 0.48822

3[PF_6]

Excited State 22: 3.012-A 2.0487 eV 605.18 nm f=0.0020 <S**2>=2.018
219A -> 229A -0.57348
206B -> 218B 0.59782
207B -> 218B 0.34945
208B -> 218B 0.40695

Excited State 23: 3.012-A 2.0496 eV 604.93 nm f=0.0032 <S**2>=2.018
219A -> 229A 0.79317
206B -> 218B 0.42571
207B -> 218B 0.26573
208B -> 218B 0.28995

Excited State 24: 3.012-A 2.0663 eV 600.02 nm f=0.0001 <S**2>=2.017
204B -> 218B -0.15131
206B -> 218B -0.49317
207B -> 218B 0.85383

Excited State 25: 3.016-A 2.0797 eV 596.16 nm f=0.0043 <S**2>=2.024
219A -> 230A 0.20701
219A -> 231A -0.18070
219A -> 232A -0.17681
219A -> 234A -0.15116
202B -> 218B 0.79284

203B -> 218B 0.38249
204B -> 218B 0.16806

Excited State 26: 3.015-A 2.1350 eV 580.73 nm f=0.0065 <S**2>=2.022
219A -> 229A 0.11560
219A -> 230A 0.59146
219A -> 231A -0.54280
219A -> 232A -0.40473
219A -> 233A -0.10025
219A -> 235A -0.20423
202B -> 218B -0.26891
203B -> 218B -0.14600

Excited State 27: 3.016-A 2.1686 eV 571.73 nm f=0.0159 <S2>=2.024**
219A -> 229A 0.10817 HOMO→LUMO+9
219A -> 230A 0.31841 HOMO→LUMO+10
219A -> 231A -0.13624
219A -> 232A 0.79196 HOMO→LUMO+12
219A -> 234A -0.27219
219A -> 235A -0.33046
200B -> 218B 0.11751

Excited State 28: 3.011-A 2.2142 eV 559.96 nm f=0.0045 <S**2>=2.016
219A -> 232A -0.13535
219A -> 234A 0.11034
199B -> 218B -0.12541
200B -> 218B 0.67234
201B -> 218B 0.15641
202B -> 218B 0.28573
203B -> 218B -0.54929
205B -> 218B -0.16810

Excited State 29: 3.015-A 2.2997 eV 539.13 nm f=0.0186 <S**2>=2.023
219A -> 232A -0.10725
219A -> 233A 0.77504
219A -> 234A -0.42667
219A -> 235A 0.15700
200B -> 218B 0.12185
201B -> 218B -0.31116
202B -> 218B -0.10153
203B -> 218B -0.10255

Excited State 30: 3.018-A 2.3478 eV 528.09 nm f=0.0257 <S**2>=2.027
219A -> 233A 0.27426
219A -> 234A -0.13596
219A -> 236A -0.13469
197B -> 218B -0.10005
199B -> 218B 0.17302
200B -> 218B -0.22905
201B -> 218B 0.84527
203B -> 218B -0.17222

Excited State 31: 3.011-A 2.3765 eV 521.71 nm f=0.0088 <S**2>=2.017
219A -> 234A 0.11832
197B -> 218B 0.25943
198B -> 218B -0.23809
199B -> 218B 0.86934
201B -> 218B -0.14037
202B -> 218B 0.10478
203B -> 218B -0.12902

```
 Excited State  32:  3.010-A      2.3866 eV  519.50 nm  f=0.0010  <S**2>=2.016
   219A -> 230A       0.64148
   219A -> 231A       0.74418

Excited State  33:  3.014-A      2.4043 eV  515.67 nm  f=0.0096  <S**2>=2.021
   219A -> 230A       0.15231
   219A -> 231A      -0.14167
   219A -> 232A       0.26603
   219A -> 233A       0.43771
   219A -> 234A       0.78134
   219A -> 235A       0.12581
   197B -> 218B      -0.10396
   203B -> 218B       0.14052

Excited State  34:  3.016-A      2.4444 eV  507.21 nm  f=0.0060  <S**2>=2.024
   219A -> 230A       0.20211
   219A -> 231A      -0.20689
   219A -> 232A       0.20562
   219A -> 233A      -0.26392
   219A -> 234A      -0.10913
   219A -> 235A       0.87310

Excited State  35:  3.012-A      2.4618 eV  503.64 nm  f=0.0063  <S**2>=2.018
   219A -> 234A      -0.11745
   219A -> 236A      -0.16750
   198B -> 218B      -0.14852
   200B -> 218B       0.60206
   201B -> 218B       0.23406
   202B -> 218B      -0.31064
   203B -> 218B       0.59939
   205B -> 218B       0.14386

Excited State  36:  3.015-A      2.5309 eV  489.88 nm  f=0.0174  <S**2>=2.023
   219A -> 228A      -0.12150
   219A -> 233A       0.14512
   219A -> 236A       0.93639
   197B -> 218B       0.10330
   200B -> 218B       0.10140
   201B -> 218B       0.16281

Excited State  37:  3.924-A      2.6400 eV  469.64 nm  f=0.0116  <S**2>=3.600
   213A -> 220A      -0.25526
   213A -> 221A       0.17200
   213A -> 223A       0.12702
   214A -> 220A       0.20045
   214A -> 221A      -0.12492
   215A -> 220A      -0.37933
   215A -> 221A       0.21936
   217A -> 220A       0.20564
   217A -> 221A      -0.10832
```

Table S9. The x,y,z Cartesian coordinates of the complex **1** calculated using Gaussian09 at B3LYP/6-31G(d,p) level and LANL2DZ for iridium in the ground state.

	X	Y	Z		X	Y	Z
C	4.6061	-0.3749	10.5217	H	2.0002	3.0571	6.4326
H	3.8181	-0.4959	11.2795	C	0.675	2.1433	7.9771
C	5.1515	-1.5585	9.8443	H	-0.1927	2.0267	7.3073
H	4.7038	-2.5445	10.0453	C	0.5938	1.723	9.3756
C	6.242	-1.427	8.8647	H	-0.3396	1.289	9.7662
C	6.707	-0.0761	8.5217	C	1.7678	1.892	10.2333
C	7.7627	0.2257	7.5422	C	1.8217	1.537	11.6492
H	8.2538	-0.5869	6.9842	C	0.7413	0.9512	12.4414
C	8.1788	1.6173	7.2931	H	-0.247	0.7563	11.9971
H	8.9673	1.8146	6.5501	C	0.9884	0.6184	13.8475
C	7.5507	2.7285	8.0249	H	0.1827	0.1771	14.4569
C	7.8938	4.1468	7.8536	C	2.3049	0.8646	14.4455
C	7.1113	5.1451	8.5999	H	2.4864	0.6033	15.5009
H	7.2511	6.2193	8.4006	C	3.3814	1.4528	13.644
C	6.0883	4.7248	9.5664	H	4.3728	1.6205	14.0906
H	5.5082	5.4848	10.1103	C	3.1239	1.8008	12.2484
C	6.0961	1.041	9.2259	C	6.8825	1.8409	12.5675
C	6.519	2.4026	8.9976	H	6.8828	0.9139	11.9759
C	6.7965	-4.5595	8.7662	C	7.9154	2.0443	13.5857
C	6.5441	-4.755	10.1977	H	8.6979	1.2836	13.7409
H	6.5045	-3.8908	10.8796	C	7.8994	3.2599	14.3992
C	6.4031	-6.1071	10.7418	H	8.6713	3.428	15.168
H	6.1919	-6.2496	11.8144	C	6.8408	4.2458	14.1835
C	6.5606	-7.2699	9.8671	H	6.8097	5.1617	14.7935
H	6.4537	-8.2876	10.2771	C	5.8355	3.9882	13.1512
C	6.8757	-7.0795	8.4507	C	4.7099	4.8686	12.8485
H	7.0135	-7.9547	7.7946	C	4.3993	6.14	13.5006
C	7.0036	-5.7274	7.9035	H	5.0209	6.5215	14.3254
H	7.2398	-5.5922	6.8352	C	3.2415	6.9126	13.0407
C	9.9947	6.2926	6.8001	H	2.995	7.8722	13.524
C	10.7195	6.8097	5.6347	C	2.4129	6.4168	11.9367
H	10.7717	6.2167	4.7068	H	1.5489	7.0074	11.5902
C	11.3588	8.1259	5.6891	C	2.7318	5.1416	11.2892
H	11.8865	8.5191	4.8047	H	2.1198	4.7818	10.4488
C	11.2936	8.9219	6.9155	C	3.8758	4.3663	11.764
H	11.7657	9.9174	6.9534	N	5.0881	0.9057	10.1887
C	10.6141	8.3875	8.0965	N	5.8365	3.3537	9.7668
H	10.587	8.9749	9.0289	N	2.9718	2.439	9.7272
C	9.9861	7.0657	8.0464	N	5.8854	2.8179	12.356
H	9.5486	6.6398	8.9633	S	6.9365	-2.8958	8.0595
C	3.0638	2.8706	8.3863	S	9.1907	4.6707	6.6997
H	3.9925	3.3281	8.0153	Ir	4.4804	2.6038	10.9875
C	1.9217	2.7257	7.4809				

Table S10. The x,y,z Cartesian coordinates of the complex **2** calculated using Gaussian09 at B3LYP/6-31G(d,p) level and LANL2DZ for iridium in the ground state.

	X	Y	Z		X	Y	Z
C	5.759	4.881	13.271	H	4.827	9.529	10.769
H	5.014	4.96	13.824	C	5.237	10.951	12.07
C	5.801	3.836	12.353	H	4.912	11.655	11.555
H	5.089	3.239	12.31	C	5.771	11.188	13.326
C	6.87	3.669	11.511	H	5.814	12.059	13.65
C	7.937	4.599	11.628	C	6.262	10.105	14.137
C	9.103	4.581	10.81	C	6.839	10.158	15.483
H	9.2	3.916	10.168	C	7.033	11.302	16.29
C	10.071	5.515	10.949	C	7.573	11.267	17.557
H	10.8	5.495	10.372	H	7.701	12.041	18.058
C	10.014	6.528	11.95	C	7.907	10.054	18.032
C	11.029	7.517	12.167	C	7.739	8.877	17.329
C	10.835	8.421	13.176	H	7.988	8.065	17.707
H	11.464	9.088	13.332	C	7.193	8.922	16.05
C	9.719	8.341	13.952	C	8.7	5.612	16.45
H	9.641	8.947	14.653	H	9.359	5.936	15.879
C	7.824	5.609	12.584	C	9.088	4.769	17.456
C	8.89	6.574	12.764	H	9.981	4.531	17.562
C	5.471	1.546	10.392	C	8.144	4.29	18.29
C	4.351	2.138	9.89	H	8.375	3.709	18.979
H	4.374	3.027	9.616	C	6.813	4.677	18.106
C	3.168	1.402	9.791	H	6.161	4.354	18.685
H	2.395	1.816	9.479	C	6.441	5.542	17.067
C	3.133	0.111	10.142	C	5.134	6.086	16.75
H	2.348	-0.381	10.048	C	3.906	5.786	17.359
C	4.269	-0.481	10.641	C	2.722	6.324	17.035
H	4.246	-1.377	10.894	H	1.935	6.087	17.471
C	5.422	0.222	10.773	C	2.744	7.246	16.013
H	6.18	-0.19	11.119	C	3.851	7.591	15.345
C	13.32	8.935	11.626	H	3.797	8.202	14.645
C	13.173	10.13	10.998	C	5.094	7.035	15.694
H	12.57	10.222	10.297	N	6.73	5.76	13.388
C	13.924	11.2	11.413	N	8.739	7.472	13.788
H	13.815	12.027	11.002	N	6.19	8.852	13.615
C	14.772	11.07	12.359	N	7.439	6.005	16.23
H	15.272	11.805	12.636	F	6.692	12.516	15.749
C	14.944	9.906	12.944	F	8.437	9.965	19.262
H	15.611	9.817	13.586	F	3.926	4.833	18.38
C	14.185	8.845	12.641	F	1.572	7.792	15.701
H	14.259	8.057	13.129	S	7.044	2.366	10.381
C	5.68	8.709	12.368	S	12.397	7.508	11.078
H	5.666	7.851	12.009	Ir	6.874	7.349	14.822
C	5.19	9.708	11.606				

Table S11. The x,y,z Cartesian coordinates of the complex **3** calculated using Gaussian09 at B3LYP/6-31G(d,p) level and LANL2DZ for iridium in the ground state.

	X	Y	Z		X	Y	Z
C	-0.06074	2.29018	-0.61628	H	1.0011	0.87997	6.55638
H	0.8751	2.66408	-1.02004	C	1.02038	-0.17898	4.66206
C	-1.18329	3.12036	-0.55041	H	0.55655	-1.07217	5.07093
H	-1.10381	4.1428	-0.89913	C	1.35703	-0.14483	3.32339
C	-2.3835	2.6231	-0.05593	H	1.18033	-1.00231	2.69537
C	-2.41018	1.264	0.39242	C	1.97709	0.99437	2.75922
C	-3.57751	0.62975	0.92706	C	3.47634	1.977	-0.44316
H	-4.49497	1.20111	1.01769	C	4.31018	2.92376	-1.07105
C	-3.56692	-0.67531	1.32239	H	4.65585	3.80468	-0.53843
H	-4.47104	-1.12496	1.71117	C	4.71816	2.72897	-2.38357
C	-2.37698	-1.46758	1.24789	H	5.36642	3.45398	-2.86633
C	-2.30072	-2.83678	1.65086	C	4.29794	1.58416	-3.07224
C	-1.06219	-3.4643	1.60284	H	4.62577	1.42096	-4.09589
H	-0.96203	-4.50447	1.89327	C	3.46772	0.64705	-2.45672
C	0.06843	-2.75853	1.17388	H	3.16334	-0.23068	-3.01722
H	1.04428	-3.23315	1.15	C	3.02637	0.82478	-1.13543
C	-1.21307	0.51093	0.30376	C	2.20462	-2.84769	-1.58419
C	-1.18572	-0.85259	0.77648	C	2.02841	-3.95764	-2.45515
C	-3.39658	5.19738	-0.54881	H	2.62348	-4.84861	-2.30068
C	-3.57845	5.52313	-1.89938	C	1.11346	-3.90384	-3.4682
H	-3.9597	4.7773	-2.59	H	0.96219	-4.75386	-4.12832
C	-3.2766	6.81145	-2.34384	C	0.37253	-2.71468	-3.6823
H	-3.41972	7.06717	-3.38963	C	-0.53981	-2.5835	-4.75808
C	-2.80151	7.76984	-1.44547	H	-0.69138	-3.43639	-5.41439
H	-2.57381	8.77298	-1.79402	C	-1.20293	-1.39685	-4.97999
C	-2.62824	7.44417	-0.09794	H	-1.89431	-1.29918	-5.81125
H	-2.26816	8.19213	0.60242	C	-0.95657	-0.29751	-4.12946
C	-2.92842	6.15922	0.35644	H	-1.45102	0.65053	-4.32162
H	-2.80968	5.90362	1.40482	C	-0.08695	-0.40141	-3.06209
C	-4.99109	-3.60511	1.15591	H	0.11539	0.45228	-2.43618
C	-6.27831	-3.37242	1.65617	C	0.5874	-1.61487	-2.79144
H	-6.42969	-3.22766	2.72201	C	3.18964	-2.83279	-0.50872
C	-7.36388	-3.33005	0.77853	C	4.10246	-3.87996	-0.27103
H	-8.3621	-3.15612	1.16977	H	4.09104	-4.7805	-0.87768
C	-7.16634	-3.49935	-0.5927	C	5.04672	-3.76264	0.73969
H	-8.01138	-3.45916	-1.27359	H	5.75508	-4.56553	0.91991
C	-5.87923	-3.72739	-1.08702	C	5.0848	-2.59623	1.51408
H	-5.72228	-3.86957	-2.15259	H	5.83091	-2.49487	2.2983
C	-4.79118	-3.79654	-0.21704	C	4.17856	-1.56022	1.28686
H	-3.79674	-4.00222	-0.60151	H	4.23698	-0.66905	1.90261
C	3.04906	2.07316	0.94837	C	3.20247	-1.65621	0.28197
C	3.38083	3.17505	1.78303	N	-0.05982	1.01783	-0.2178
H	3.9463	3.99959	1.36805	N	0.02016	-1.49029	0.77021
C	2.98377	3.1969	3.09007	N	2.31674	1.03529	1.41638
H	3.22023	4.04246	3.73063	N	1.45958	-1.72563	-1.72082
C	2.28118	2.09043	3.62861	S	-3.87575	3.57397	0.04663
C	1.90646	2.03407	4.99371	S	-3.64891	-3.7781	2.34198
H	2.14046	2.88371	5.62967	Ir	1.74186	-0.33721	-0.11952
C	1.27912	0.92108	5.50786				

References

1. A. M. Brouwer, *Pure Appl. Chem*. 2011, **83***,* 2213–2228.

2. V. V. Pavlishchuk and A. W. Addison, *Inorg. Chim. Acta* 2000, **298**, 97–102.

3. A. D. Becke, *J. Chem. Phys*. 1993, **98***,* 5648–5652.

4. P. J. Hay and W. R. Wadt, *J. Chem. Phys*. 1985, **82**, 270–283.

5. M. Cossi and V. *J.* Barone, *Chem. Phys*. 2001, **115**, 4708–4717.